Cluster Models of Cu Binding and CO and NO Adsorption in Cu-Exchanged Zeolites

W. F. Schneider* and K. C. Hass*

Ford Research Laboratory, MD 3083/SRL, Dearborn, Michigan 48121-2053

R. Ramprasad and J. B. Adams

Department of Materials Science and Engineering, University of Illinois, Urbana, Illinois 61801

Received: August 1, 1995; In Final Form: October 23, 1995[⊗]

A small cluster model is proposed and used to examine the properties of bound Cu ions and their interactions with CO and NO in Cu-exchanged zeolites, such as Cu−ZSM-5. The model uses H_2O ligands to represent the framework oxygens of the zeolite lattice that form the local coordination environment of the Cu ion. Variations in the oxidation state of the metal center are simulated by adjusting the net charge on the clusters. Density functional theory is used to predict the molecular and electronic structures and binding energies of these model clusters, including $Cu(H_2O)_x^{n+}$, $Cu(H_2O)_xCO^{n+}$, and $Cu(H_2O)_xNO^{n+}$ ($x = 1-4$, $n = 0-2$). While quite simplistic, this model provides considerable insight into the behavior and interactions of zeolite-bound Cu ions. Both Cu^+ and Cu^{2+} ions are found to bind strongly to H_2O (or bridge oxygen) ligands, with Cu^{2+} preferring higher and Cu^+ preferring lower coordination numbers. CO and NO also bind strongly to both Cu ions. Cu^{2+} preferentially binds the three ligands in the order $Cu^{2+}-NO > Cu^{2+}-OH_2 > Cu^{2+}-CO$ while Cu^+ exhibits an almost equal affinity for the three. Bare Cu^0 is weakly bound to H_2O and is unlikely to be stable within a zeolite, but both $CuCO^0$ and $CuNO^0$ may exhibit some stability as products of reduction processes. The $Cu-OH_2^{n+}$ and $Cu-CO^{n+}$ interactions are primarily electrostatic, but the $Cu-NO^{n+}$ interactions have a large covalent component that complicates their electronic structures and makes assignment of Cu oxidation states difficult. Three modes of NO binding on Cu are predicted, represented approximately as $[Cu(I)-(N{\equiv}O)^+]$, $[Cu(I)-(N{\equiv}O^\bullet)]$, and $[Cu(I)-(N{\equiv}O)^-]$. The implications of these results for understanding Cu-exchanged zeolites is discussed, as are the limitations and possible extensions of the H_2O ligand model.

Introduction

Cu zeolites, in particular Cu−ZSM-5, display unusually high activities for the catalytic decomposition of NO into N_2 and O_2[1,2] and for the selective catalytic reduction (SCR) of NO by hydrocarbons in the presence of excess oxygen.[3,4] Because of interest in their potential application as lean-NO_x automotive catalysts, considerable research has been directed at understanding and improving these materials.[5] Despite this interest, fundamental questions about the nature of the active sites in such catalysts and the precise catalytic mechanisms remain. In an attempt to address some of these questions, we have begun a computational investigation of model Cu complexes in ligand environments similar to what might be found in Cu-exchanged zeolites, with an initial emphasis on understanding the structure and energetics of NO and CO bound to Cu.

A major difficulty in trying to model the chemistry at exchanged transition metal ion sites in zeolites is that the exact location of these ions is often unknown. In many cases, such as ZSM-5, a variety of sites may be possible, and these may vary with temperature, transition metal ion oxidation state, and the presence of other species either bound to the ion or in nearby pores.[6] The framework structures of most zeolites are themselves complicated, containing both SiO_4 and AlO_4 corner-sharing tetrahedra in generally disordered arrangements over large-unit-cell crystalline networks. Before ion exchange, extralattice protons or alkali ions are usually present to compensate the negative framework charge that is introduced by each AlO_4 unit. A proton of this kind is well-known to be bound to a single "bridge" oxygen between an aluminum and

a silicon (a so-called Brønsted acid site). By contrast, exchanged transition metal ions such as Cu tend to coordinate simultaneously to several framework oxygen, most likely still in the vicinity of one or more aluminums.[6,7] In many zeolites, the locations of such exchanged ions have been directly determined by X-ray or neutron diffraction. [8] No such results have yet been reported for Cu−ZSM-5, most likely because of the relatively high Si/Al ratios (>15), and hence low Cu concentrations, in the materials of greatest practical interest. What little is known about the location of Cu ions in ZSM-5 has been deduced from indirect spectroscopic measurements.[9−14] For example, electron spin resonance (ESR), which detects only Cu^{2+}, provides evidence for at least two distinct sites in dehydrated ZSM-5; these two are often referred to as "square planar" and "square pyramidal," although their exact nature is unclear.[10,11] Other measurements,[12−14] such as X-ray absorption near edge spectroscopy (XANES) and extended X-ray absorption fine structure (EXAFS), support the notion of highly coordinated Cu^{2+} in ZSM-5 and indicate a somewhat lower average coordination for Cu^+.

The dependence of Cu oxidation state on sample history and reaction conditions in Cu zeolites is also not well understood. Iwamoto et al.[1] originally proposed a cyclic redox mechanism for NO decomposition by Cu−ZSM-5, which begins with a spontaneous thermal reduction of Cu^{2+}. This reduction process has proven to be highly controversial,[15,16] and recent ESR studies suggest that it does not always occur.[17] Shelef instead argues in favor of a dinitrosyl coupling mechanism for NO decomposition which involves only Cu^{2+} sites.[5,15] The oxidation state and role of Cu sites active in the selective catalytic reduction of NO are even more unclear. Unambiguous experimental evidence exists for both Cu^{2+} and Cu^+ ions in ZSM-5 and other

---

* Authors to whom correspondence should be addressed.
⊗ Abstract published in *Advance ACS Abstracts,* March 15, 1996.

Cluster Models of Cu-Exchanged Zeolites

J. Phys. Chem., Vol. 100, No. 15, 1996 **6033**

zeolites, but their relative activities are often difficult to separate from other issues such as the Cu-loading and feed gas composition.[13b,14,17b] A further complication is the fact that a single framework aluminum can be charge compensated by a bare Cu^+ ion, while two framework aluminums are required to compensate a bare Cu^{2+}. It has therefore been suggested that, at high Si/Al ratios, the aluminum centers may be too far apart on average to bind a dication and that some or all Cu^{2+} may be present as an extralattice $[Cu^{2+}OH^-]$ complex compensating a single framework aluminum.[5,18] This description is consistent with the observation that even under conditions in which one expects to find only Cu^{2+}, many Cu−ZSM-5 samples are nevertheless "overexchanged", that is, contain more than one Cu^{2+} cation for every two Al atoms.

In this work, we attempt to provide general insight into the properties of bound Cu ions and their interactions with NO and CO in Cu-exchanged zeolites. To this end, we present a density functional theory[19] study of a series of simple cluster models containing Cu^{n+} ions ($n = 0-2$) in zeolite-like ligand environments of varying coordination. The specific models we consider use water ligands to represent the coordination of Cu^{n+} to framework oxygen. While this model is clearly an oversimplification of the environment in real zeolites, the use of water ligands mimics the dominant nearest-neighbor contributions to the ionic ligand field while keeping the overall problem to a computationally manageable size. The water ligand models are amenable to more rigorous computational tools than are larger zeolite models containing explicit tetrahedral (Si or Al) sites. The simplicity and flexibility of this approach allows one to consider easily a wide range of model geometries, thus facilitating the systematic investigation of structural and energetic trends. Such an approach is particularly warranted in the case of Cu-exchanged zeolites because of the limited experimental information available on Cu binding sites.[7] While we do not expect the water ligand model predictions to be quantitatively accurate for real zeolites, we do expect the extracted qualitative trends (e.g., a preference for high oxygen coordination number) to be relatively robust. Of course, the actual coordination geometry in a particular zeolite is also influenced by the zeolite topology and the location of aluminum, neither of which is included in the water ligand model. Most other approximations in the model, such as the neglect of long-range electrostatic and strain fields, are common to most quantum-mechanical studies of zeolites.[20] A few more specific issues, such as the consideration of charged clusters instead of neutral ones with counter charges, are discussed briefly at the end of the Results and Discussion section.

The simple water ligand model is motivated primarily by the opportunities it affords for studying the chemistry at exchanged Cu sites. Here we use this model to investigate the binding of CO and NO to Cu^{n+} ($n = 0-2$) ions with varying oxygen coordination. CO may be an important intermediate in the SCR reaction, and CO has been used as a spectroscopic probe to elucidate the nature of the Cu sites in ZSM-5.[1c,21] Further, the interaction of CO with metal atoms is well understood, and thus it is a useful computational as well as spectroscopic probe. The interaction of NO with Cu binding sites has obvious relevance to both the decomposition and SCR reactions. The binding of NO to transition metal ions is more complex than CO,[22] and while considerable spectroscopic information is available for these systems, its interpretation is not unambiguous. As with the binding of Cu itself, we attempt here to obtain qualitative information about the interaction of a Cu ion with CO and NO, along with an understanding of how this interaction is modified by incorporating the Cu ion into a field of framework-oxygen-

TABLE 1: Comparison of Calculated and Experimental Molecular Parameters for CO, NO, and H_2O

	CO	NO	H_2O
molecular geometries[a]			
LSDA	r_{CO}: 1.131	r_{NO}: 1.154	r_{OH}: 0.980
			$\angle_{HOH}$: 104.5
exp	1.128[b]	1.151[b]	0.958[c]
			104.5
atomization energies[d]			
LSDA	294.7	191.0	251.5
BP86	270.6	164.1	230.6
exp[c]	256.4	149.8	219.3
harmonic vibrational frequencies[e]			
LSDA	2186	1941	a_1: 1574, 3679
			b_2: 3772
exp	2170[b]	1904[b]	a_1: 1653, 3825
			b_2: 3936[f]

[a] Distances in angstroms and angles in degrees. [b] Reference 62. [c] Reference 63. [d] Energies in kcal mol^{−1}. Calculations referenced to spherical atoms and corrected for zero point energy using LSDA frequencies. [e] Frequencies in cm^{−1}. [f] Reference 64.

like ligands. The computational results do provide valuable new insights into the Cu−CO and Cu−NO interactions and in particular into their sensitivity to Cu oxidation state and coordination environment.

Computational Details

Calculations were performed using the Amsterdam Density Functional code, ADF.[23] Geometries were obtained by gradient optimizations[24] within the local (spin) density approximation [L(S)DA],[25] followed by single-point energy calculations using the gradient-corrected Becke exchange[26] and Perdew correlation[27] [BP86] functionals. Binding energies were examined using the "transition state" method, which provides a breakdown of the overall binding energy in terms of electrostatic and orbital contributions.[28] A limited number of calculations were performed using the full gradient-corrected potentials in the optimization procedure.[29] In general, the gradient corrections tend to increase the optimized bond lengths uniformly, but in all cases examined BP86 binding energies calculated at the LDA and BP86 geometries differ negligibly. The ADF code employs Slater-type basis functions for expansion of the molecular orbitals and charge density. A split-valence plus polarization molecular orbital basis set was used for all atoms save Cu, for which a triple-zeta d orbital representation was used. Atomic core orbitals were frozen in all calculations, including the 1s orbitals for C, N, and O and the 1s, 2s, and 2p orbitals for Cu. ADF employs a large charge density basis, and the charge fitting errors are uniformly small. The molecular grid used to perform numerical integration within ADF is controlled by a single accuracy parameter.[30] An integration parameter of 3.5 was used in the geometry optimization calculations and a value of 4.0 for the single-point calculations. These integration meshes were found to be more than sufficient to ensure convergence of geometries and energies to the precision quoted in this work.

For reference against the larger Cu-containing clusters, and as simple benchmarks of the methods employed here, Table 1 contains comparisons of the calculated and experimental geometric, energetic, and vibrational properties of CO, NO, and H_2O. The LDA method performs very well for both the structures and vibrational spectra, but systematically overestimates the atomization energies. The BP86 functional also overestimates these energies, but by a smaller margin. As will be shown below, BP86 predictions for the binding energies of

molecular fragments within larger clusters are significantly more accurate than these difficult to calculate homolytic dissociation energies.

Many of the preliminary calculations on the four-water models were performed using the DMol density functional program.[31] The results of these calculations are entirely consistent with those from the ADF program reported here.

Results and Discussion

I. $Cu(H_2O)_x^{n+}$ Models. We first examine the coordination preferences of otherwise unligated Cu ions within a zeolite by calculating the binding energy, geometry, and electronic structure as a function of metal coordination number and oxidation state. Water ligands are employed as surrogates for the zeolite bridge oxygens, and water-ligated Cu complexes of various coordination numbers, symmetries, and overall charges are constructed to represent zeolite-bound Cu ions. We will briefly examine extensions of the H_2O model at the end of the Results and Discussion.

An important question in the chemistry of Cu−ZSM-5 is the oxidation state of the active Cu species. The oxidation state of a metal center can be difficult to assign unambiguously, particularly in an environment as complex as a zeolite. Nonetheless, the oxidation state is a useful concept for qualitative discussions of bonding. In this work, we carefully distinguish between the net charge on a system, which is applied as input to a given model compound, and the resultant Cu oxidation state, which is determined by examination of molecular orbitals and Mulliken populations. The notation Cu^0, Cu^+, and Cu^{2+} is used to refer generically to neutral, monopositive, and dipositive atoms and clusters, while the notation Cu(0), Cu(I), and Cu(II) is used to refer to Cu atoms in approximately the 0 ($d^{10}s^1$), 1+ (d^{10}), and 2+ (d^9) oxidation states, respectively. In the $Cu(H_2O)_n^{x+}$ clusters examined here, the overall cluster charge and the effective Cu oxidation state are the same. In the $Cu(H_2O)_nCO^{x+}$ and $Cu(H_2O)_nNO^{x+}$ clusters examined later on, the two do not correspond directly, and the distinction between the cluster charge and approximate Cu oxidation state is carefully noted.

The clusters examined include Cu ions coordinated to up to five water molecules, i.e., $Cu(H_2O)_x^{n+}$, ($x = 1-5$, $n = 0-2$), as models of 1- to 5-coordinated, monodispersed Cu ions within a zeolite lattice. Monodispersed Cu^0 is unlikely to be present in Cu−ZSM-5, but clusters of fully reduced Cu are present under some treatment conditions. The results on the monometallic Cu^0 systems provide crude models of Cu^0 clusters and are also useful for comparison with the Cu−CO and Cu−NO systems, where the formally 0 oxidation state may be important.

Geometries. In the model used here, a Cu binding site in a zeolite is envisioned as a Cu ion coordinated to the aluminosilicate framework through an approximately equatorial band of sp^3-hybridized bridge oxygen atoms. The zeolite may also provide additional axial coordination, or axial coordination sites of the ion may be occupied by extralattice species or be vacant. The zeolite lattice relaxes locally to accommodate the bound ion,[32] but the essential lattice structure remains intact. The Cu−H_2O cluster models are constructed to simulate this type of coordination picture. Symmetry constraints are employed to maintain "zeolite-like" coordination, and full geometry optimizations within these constraints are used to approximate the relaxation of the zeolite lattice. Figure 1 contains representative sketches of the various Cu−H_2O cluster geometries considered. In the one-coordinate case, which in our model corresponds to a Cu ion bound to a single bridge site within a zeolite, both planar (C_{2v}) and pyramidal (C_s) geometries were examined;
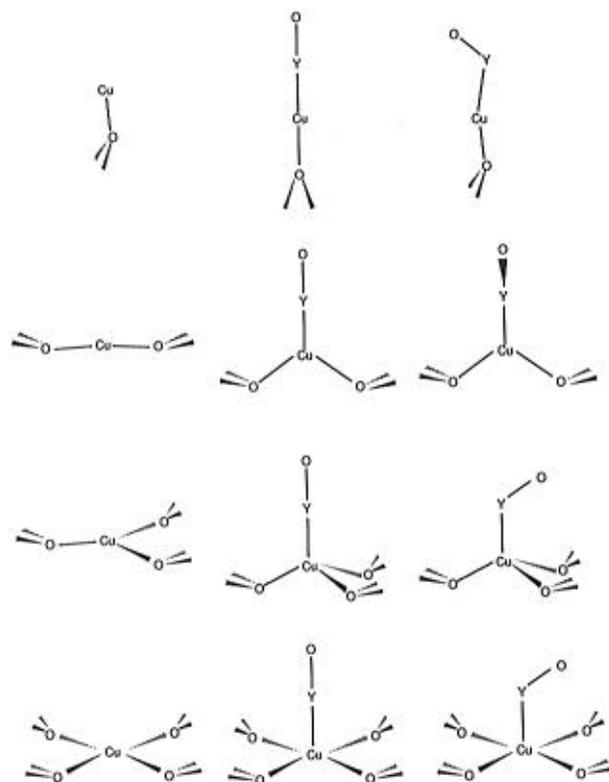

Figure 1. Molecular structures used in the $Cu(H_2O)_x^{n+}$ calculations (first column), the linearly coordinated CO and NO structure calculations (second column), and the bent CO and NO structure calculations (third column).

while both types of minima were found, they differed very little in energetic and qualitative features, and we report only the lower energy C_s results. In the two-, three-, and four-coordinate cases, the clusters are optimized under the constraint of C_{xv} symmetry, with $x = 2$, 3, or 4, respectively, and with the water ligands pyramidalized at the oxygens. Finally, in the five-coordinate case, a square-pyramidal geometry is constructed from the four-coordinate model by the addition of an axially coordinated water ligand. For simplicity, the axial water is constrained to be planar to preserve C_{2v} symmetry.

In all these cases it is possible to locate an LDA energy minimum satisfying the prescribed geometry constraints. These model structures are in general not global minima on their respective potential energy surfaces. In fact, in many cases they are saddle points with respect to relaxation of the symmetry constraints, for instance toward rotation of the H_2O ligands. The purpose here is to construct generic models of Cu coordination within zeolites, not of Cu−H_2O complexes. That the Cu−H_2O structures reported here are not global minima, or are not necessarily minima at all, has no consequence for their use as models of Cu−ZSM-5.

Table 2 contains the LDA-optimized results for the Cu−H_2O complexes in the five-coordination geometries considered. Not surprisingly, as the charge on the system decreases, the optimal Cu−O bond length tends to increase, for example from 1.964 Å in $Cu(H_2O)_4^{2+}$ to 2.116 Å in $Cu(H_2O)_4^+$ to 2.145 Å in Cu-$(H_2O)_4$. These optimal distances are not unreasonable for coordination of a Cu ion within a zeolite; for instance, the distance from the center of a six-membered ring in ZSM-5 to the four nearest oxygen centers is approximately 2.27 Å, only slightly larger than the calculated relaxed distances in the water model. For a given overall charge, the optimal geometric parameters vary over approximately 0.20 Å as the coordination number is changed. In each case, the optimal Cu−O bond

TABLE 2: Selected LSDA Optimized Geometric Parameters and Mulliken Charges and LSDA and BP86 Binding Energies of $[Cu(H_2O)_x]^{n+}$ Complexes

	geometry[a]		Mulliken Charge	binding energy[b]	
	r(C−O)	∠O−Cu−X[c]	Cu	LSDA	BP86
$n = 2$[d]					
$x = 1$	1.906		1.460	−139.5	−126.0
$x = 2$	1.871	78.1	1.292	−231.8	−205.4
$x = 3$	1.938	96.3	1.122	−286.5	−248.9
$x = 4$	1.964	85.9	1.029	−341.4	−293.3
$x = 5$	2.113 (eq)	110.2	0.924	−372.7	−316.1
	1.989 (ax)				
$n = 1$					
$x = 1$	1.888		0.826	−52.3	−39.4
$x = 2$	1.855	87.1	0.677	−105.6	−79.1
$x = 3$	1.969	87.5	0.578	−124.9	−91.1
$x = 4$	2.116	86.3	0.486	−130.8	−93.2
$x = 5$	2.085 (ax)	110.2	0.430	−147.6	−103.2
	2.189 (eq)				
$n = 0$					
$x = 1$	2.062		−0.088	−12.4	−2.8
$x = 2$	1.996	84.9	0.022	−21.7	−0.3
$x = 3$	2.006	89.7	0.135	−32.8	+0.1
$x = 4$	2.145	88.3	0.275	−36.4	+1.5

[a] Distances in angstroms and angles in degrees. [b] Energy of reaction $Cu^{n+} + xH_2O \rightarrow [Cu(H_2O)_x]^{n+}$, in kcal mol^{-1}. [c] Angle between Cu−O vector and vertical axis of symmetry. [d] Binding energy referenced to spherically averaged Cu^{2+} ion.

distance decreases when a second water is added, but increases as third and fourth waters are added, with the biggest variation in Cu−O bond distance found for Cu$^+$. Hartree−Fock calculations on similar Cu$^{+\,33,34}$ and Cu$^{0\,35}$ systems yield the same qualitative trends, but much longer absolute bond lengths, while HF calculations on one- and two-coordinate Cu^{2+} agree reasonably well with the LDA results.[36] A limited number of geometry optimizations performed using gradient-corrected exchange-correlation functionals yield Cu−O bond lengths that are intermediate between the LDA and Hartree−Fock results, but in all cases the LDA length trends are reproduced.

In almost all cases in the water models the Cu ion chooses a location between the planes defined by the oxygen centers and the hydrogen centers. The one exception is Cu(H$_2$O)$_3^{2+}$, where the Cu ion resides above both the oxygen and hydrogen planes. The greater pyramidalization at Cu in this case arises from strong mixing between the high lying, partially occupied $d_{x^2-y^2,xy}$ and $d_{xz,yz}$ orbitals permitted under C_{3v} symmetry.

Addition of a fifth axial water ligand to the four-coordinate model causes the Cu ion to be drawn above the plane of the equatorial ligands. The same qualitative behavior is expected within a zeolite lattice, where otherwise unligated Cu ions will not sit at the center of an oxygen ring but will be drawn into the zeolite framework to maximize coordination to the lattice. Conversely, extralattice ligands such as H$_2$O, CO, or NO will tend to pull a Cu ion above the plane of the oxygen coordination site.

Electronic Structure. The electronic structures of the Cu−H$_2$O complexes are well described in terms of a primarily electrostatic, ion-dipole interaction between water ligands and a Cu ion in an oxidation state equal to the overall charge of the cluster. As examples, molecular orbital diagrams for Cu(H$_2$O)$_x^+$ ($x = 1-4$) are presented in Figure 2. The atomic Cu$^+$ ^{1}S (d^{10}) electron configuration is evident in the highest energy orbitals of the complexes, and these predominantly d orbitals are split in fashions characteristic of the particular coordination geometries. In the four-coordinate case the d orbitals exhibit the characteristic square-planar crystal field splitting of one orbital above four, and in the 3-fold case the characteristic two above
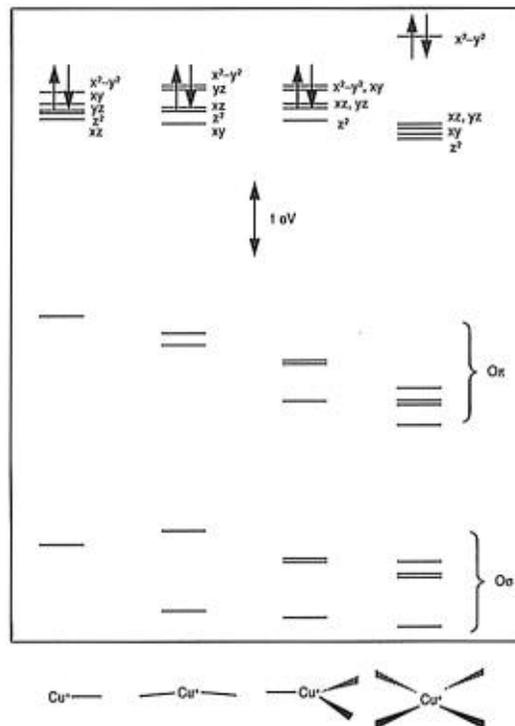

Figure 2. Molecular orbital diagrams for Cu(H$_2$O)$_x^+$, $x = 1-4$. For ease or interpretation, the orbitals are shifted vertically so that the centroids of the d bands are approximately the same energy.

three trigonal splitting is evident. The molecular orbital analysis is essentially unchanged for the other net charges and oxidation states. Thus, atomic Cu^{2+} has a ^{2}D (d^9) ground electronic configuration, and these d orbitals are split by the oxygen crystal field just as in the Cu$^+$ case. As a result, C_{3v} Cu(H$_2$O)$_3^{2+}$ has a Jahn−Teller-active (^{2}E) ground state. The structural consequences of the Jahn−Teller activity have not been examined in detail. Similarly, Cu^0 has a ^{2}S (d^{10}s^1) ground configuration, and the high-energy 4s orbital remains the highest occupied orbital in the Cu^0 water complexes. Mulliken population analysis confirms that, in both the Cu^{2+} and low-coordinate Cu^0 cases, the majority of the spin density resides on the Cu center. The relative energies of the d levels and the oxygen p manifold do vary with the formal oxidation state of the Cu ion, so that in the Cu^0 case the metal and oxygen levels are well separated, in the Cu$^+$ case they approach more closely, and in the Cu^{2+} case they are strongly mixed. These interactions further contribute to the ligand field splitting of the Cu d levels.

Mulliken population analyses (Table 2) are consistent with the characterization of the Cu$^+$−OH$_2$ and Cu^{2+}−OH$_2$ bonding as primarily electrostatic: in both oxidation states, the Cu d orbital populations are insensitive to coordination number, and the Cu gross charge decreases only a small amount (0.10 e) as each water is added, indicating only a small amount of charge transfer from ligands to metal. The Cu^0 case exhibits the opposite trend, with the metal charge increasing with increasing coordination number. The Cu 4s electron is weakly bound, and the increasing Cu charge reflects increasing donation of the 4s charge density to the ligands with increasing coordination.

The qualitative features of this electronic structure analysis are expected to carry over to actual zeolite systems. Binding of the Cu ions to the zeolite framework will occur primarily through electrostatic interactions, with secondary orbital interactions between oxygen p and metal ion d levels. Because of the importance of electrostatics, Cu ions in real zeolites will be strongly attracted to framework oxygens in negatively charged regions near Al-substituted sites. This localized attraction will

6036 *J. Phys. Chem., Vol. 100, No. 15, 1996*

Schneider et al.

provide an additional perturbation on the geometries, electronic structures, and binding energies of exchanged Cu ions, as well as their interactions with CO and NO. Nonetheless, we expect the qualitative trends predicted by the simple water model to be preserved. Further, the results in the next section suggest that both Cu^+ and Cu^{2+} can bind strongly to a zeolite framework without aluminum immediately adjacent, although proximity to aluminum is clearly desirable. The relatively large separations between aluminum atoms at high Si/Al ratios are thus not necessarily inconsistent with the binding of bare Cu^{2+}.

Binding Energies. Table 2 also contains the LSDA and BP86 binding energies for formation of the Cu–H_2O complexes from isolated Cu ions or atoms and water molecules. In general, the absolute binding energies increase with the Cu charge, as one would expect for an interaction dominated by electrostatic effects. Thus, Cu^{2+} strongly binds up to five water molecules, Cu^+ binds up to five but more weakly, and Cu^0 binds more than one water weakly (at the LSDA level) or not at all (at the BP86 level). The LSDA binding energies are uniformly greater than the gradient-corrected results, by approximately $10-12$ kcal mol^{-1} per water molecule. We refer to the BP86 results in all subsequent discussions of the binding energies.

Energy decomposition[28] of the binding energies of $Cu(H_2O)_4^+$ and $Cu(H_2O)_4^{2+}$ supports the characterization of the Cu–OH_2 interaction as primarily electrostatic, with 74% and 58% of the gross binding energy coming from electrostatic contributions, respectively. The smaller electrostatic contribution in the more highly charged system is consistent with the electronic structure analysis presented above: the d orbitals of Cu^{2+} are closer in energy to the H_2O oxygen levels, and the orbital interactions (and bonding) are relatively greater in this case. The effect of basis set superposition error (BSSE) on the gradient-corrected energies has been estimated using the counterpoise method.[37] The BSSE is greatest in the Cu^{2+} case and ranges from approximately 1 kcal mol^{-1} for CuH_2O^{2+} to 6 kcal mol^{-1} for $Cu(H_2O)_4^{2+}$. For the qualitative discussions presented here, this error is negligible, and it is not systematically corrected for in any of the binding energies reported here.

Both experimental[38-40] and ab initio computational[33,34] results for successive binding of H_2O to Cu^+ have previously been reported. Agreement between these earlier results and those reported here is excellent (within 3 kcal mol^{-1}, compared to the best experiments[40] and calculations[34b]) for the first three binding energies. Our calculated fourth binding energy is 10 kcal mol^{-1} less than the experimental result, a discrepancy that disappears when our model square planar geometry is replaced with the experimental tetrahedral one. This remarkable level of agreement, while reassuring, is in part fortuitous, given the neglect here of zero-point vibrational energy and BSSE, among other factors. Agreement between ab initio calculations on one- and two-coordinated Cu^{2+} [33,36] and the present work is not quite as impressive, with discrepancies as large as 30 kcal mol^{-1} for the first binding energy. No experimental data are available for the Cu^{2+} systems, so the relative accuracies of the calculations cannot be assessed. Clearly, further work is needed to resolve the discrepancies. We believe the BP86 binding energy results to be more than adequate for the qualitative analyses reported here.

Table 3 presents the BP86 binding energies in a more suggestive format useful for consideration of binding within zeolites. The second column of Table 3 contains the incremental energies for successive additions of H_2O ligands to the Cu ions. In general, the incremental binding energies are found to decrease as the number of substituents increases. For Cu^+, the first and second added waters are each bound by almost 40 kcal

TABLE 3: BP86 Binding Energies for Addition of H_2O, CO, or NO to $[Cu(H_2O)_x]^{n+}$ Complexes, in kcal mol^{-1}

	$+H_2O$	$+CO$	$+NO$
Cu^{2+}	-126	-98	-158
$Cu(H_2O)^{2+}$	-79	-60	-100
$Cu(H_2O)_2^{2+}$	-44	-42	-66
$Cu(H_2O)_3^{2+}$	-44	-31	-56
$Cu(H_2O)_4^{2+}$	-23	-12	-23
Cu^+	-39	-39	-33
$Cu(H_2O)^+$	-40	-42	-34
$Cu(H_2O)_2^+$	-12	-20	-16
$Cu(H_2O)_3^+$	-2^a	-22	-14
$Cu(H_2O)_4^+$	-10	-19	-17
Cu^0	-3	-13	-26
$Cu(H_2O)^0$	2	-15	-36
$Cu(H_2O)_2^0$	0	-20	-38
$Cu(H_2O)_3^0$	1	-17	-39
$Cu(H_2O)_4^0$		-16	-41

^{a} Energy to form a square-planar complex. Tetrahedral $Cu(H_2O)_4^+$ is 8 kcal mol^{-1} more stable.

mol^{-1}, while the third and fourth are bound by a total of only 14 kcal mol^{-1}. Cu^+ is known to form primarily low-coordinate (four or fewer ligand) complexes,[41] and two-coordinate, linear structures are thought to be particularly stable because of the availability of favorable sd metal hybridization.[34b,38] These binding energies are somewhat sensitive to the chosen coordination geometry, but the general trends are constant. For instance, tetrahedral $Cu(H_2O)_4^+$ is more stable than square planar $Cu(H_2O)_4^+$, but only by 8 kcal mol^{-1}. Extrapolating these results to Cu-exchanged zeolites, we expect Cu^+ to strongly bind to at least two bridge oxygens. Higher coordination sites are energetically preferred, but only by a relatively small margin, and will be entropically less favorable. As we will show below, this preference for relatively low-coordination geometries persists when CO or NO is added to Cu^+.

In contrast, the incremental H_2O binding energies for Cu^{2+} are all very large, with the fourth water ligand bound by 44 kcal mol^{-1} and the fifth by 23 kcal mol^{-1}. Cu^{2+} is known to prefer to form high-coordinate complexes with small ligands in aqueous solution, including the nearly octahedral $Cu(H_2O)_6^{2+}$.[41] In zeolites, we infer that Cu^{2+} will have a strong preference for high-coordination sites and in hydrated samples will have a large affinity for extralattice H_2O. These preferences are consistent with ESR and other experimental data on Cu-exchanged zeolites, including ZSM-5.[7,9,10] This preference for high coordination numbers persists when either CO or NO is bound to Cu^{2+}.

Finally, the calculations indicate that Cu^0 is only very weakly bound to one water and can bind no more than that. Energy decomposition analysis indicates that the binding is primarily electrostatic, arising from partial charge transfer from Cu to H_2O, with only a small (28%) orbital relaxation contribution. Cu^0 is not expected to interact strongly with a zeolite host.

II. $Cu(H_2O)_xCO^{n+}$ Models. CO is both adsorbed by and active in the chemistry of Cu-exchanged zeolites. High-temperature treatment of Cu^{2+}-exchanged zeolites with CO results in reduction of the metal atoms to Cu^+, and binding of CO to Cu sites within zeolites is well-known.[42] CO is known to be a (nonselective) reductant for NO over Cu–ZSM-5,[3] and CO may play a role in the selective catalytic reduction of NO. Further, CO is a sensitive spectroscopic probe for examination of binding sites; it has a distinct, readily detectable infrared absorption feature that is highly sensitive to its coordination environment.

For these reasons, and because the binding of CO to metal atoms is better understood than the binding of NO, it makes
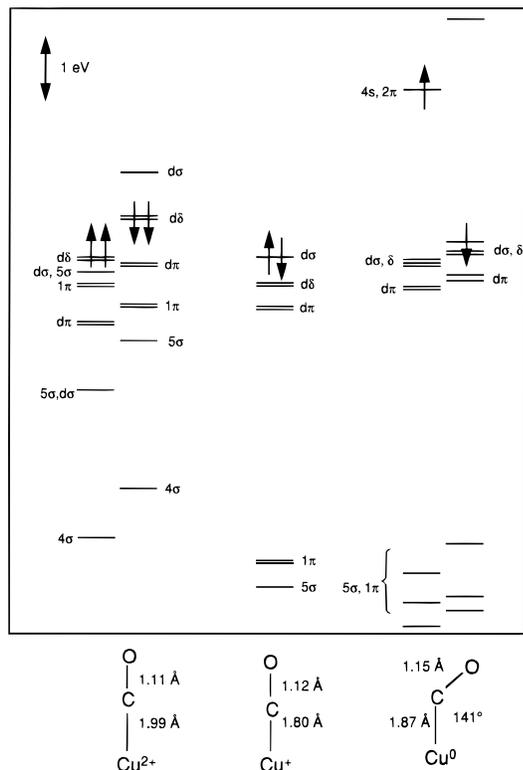
Cluster Models of Cu-Exchanged Zeolites

J. Phys. Chem., Vol. 100, No. 15, 1996 **6037**

Figure 3. Molecular orbital diagrams for CO on bare Cu atom and ions. For ease of interpretation, the orbitals are shifted vertically so that the tops of the spin-up d orbital manifolds have the same energy.

sense to consider first the binding of CO to zeolite-bound Cu ions. For this purpose we build upon the Cu$-$H$_2$O models by introducing a CO ligand in the vacant axial coordination site and investigate the energetic and structural trends as a function of cluster charge and coordination number. Before discussing the Cu$-$H$_2$O$-$CO model results, however, it is constructive to consider CO binding to otherwise unligated Cu ions.

CuCO^{n+}. Table 4 contains geometry and energy results for CuCO^{n+} ($n = 0, 1, 2$), and Figure 3 contains molecular orbital diagrams for the three. The binding of CO to metal ions is usually described in terms of donation from the occupied, antibonding 5σ orbital of CO into vacant metal orbitals and back-donation from occupied metal d orbitals into the vacant, antibonding CO 2π orbitals.[41] These two interactions have opposite effects on the C$-$O bond length and strength, the former tending to shorten and strengthen the bond and the latter tending to lengthen and weaken it. The two are conveniently represented by the following resonance structures:

$$M\leftarrow C\equiv O \leftrightarrow M=C=O$$

The relative efficiency of these two modes is controlled by the spatial and energetic match between the metal and CO orbitals. The effects of σ donation and π back-donation are evident in the molecular orbital diagrams in Figure 3: the σ donation resulting in destabilization of the dσ orbitals and the π back-donation resulting in a stabilization of the dπ orbitals. The magnitudes of these interactions vary considerably with the net charge, with the greatest amount of orbital interaction found in the Cu^{2+} case, followed by Cu$^+$ and lastly Cu^0.

CO has an experimental bond length of 1.128 Å, which is reasonably well reproduced at the LDA level of theory used here (1.131 Å, Table 1). CO binds to Cu^{2+} in a linear fashion, strongly mixing with and splitting the Cu d orbitals to generate a (d$_{z^2}$)^1 ($^2\Sigma^+$) ground state. The calculated C$-$O bond length decreases by 0.019 Å relative to the free molecule, suggesting that σ donation from CO to Cu^{2+} dominates the Cu$^{2+}-$CO

interaction. The Cu$^{2+}-$CO bond energy is calculated to be 98 kcal mol^{-1}. While large, this binding energy is considerably less than that found for the Cu$^{2+}-$OH$_2$ bond. Further, the calculated Cu$^{2+}-$CO bond length is 0.08 Å greater than the Cu$^{2+}-$OH$_2$ bond length. These results are consistent with a large electrostatic contribution to bonding to Cu^{2+}, with the greater polarity of H$_2$O relative to CO resulting in the stronger Cu$^{2+}-$OH$_2$ bond. As we shall see, the preference for H$_2$O ligands over CO persists in the larger models incorporating both H$_2$O and CO ligands.

While CuCO^{2+} is strongly bound with respect to fragmentation into Cu^{2+} and CO, it is in fact unbound (by 65 kcal mol^{-1}) with respect to separation into Cu$^+$ and CO$^+$. In other words, a bare Cu^{2+} ion is capable of oxidizing CO, and CuCO^{2+} is not a stable species. Addition of H$_2$O ligands decreases the oxidizing power of Cu^{2+} and stabilizes (H$_2$O)$_x$Cu$-$CO^{2+} against loss of CO$^+$. The dissociative behavior of CuCO^{2+} is similar to that of CuNO^{2+}, which is discussed in greater detail later in the Results and Discussion.

Cu$^+$ also prefers polar ligands, although the preference is not as great as in the Cu^{2+} case. Cu$^+$ has a d^{10} (^{1}S) ground configuration and binds CO in a linear fashion, yielding a $^1\Sigma^+$ ground state.[43,44] The C$-$O bond length decreases relative to free CO by 0.010 Å at the LDA level, again suggesting that σ donation is more important than π back-donation in the bonding interaction. Ab initio calculations including electron correlation predict a similar decrease in C$-$O bond length.[43] The BP86 Cu$^+-$CO bond energy (39 kcal mol^{-1}) agrees well both with these ab initio calculations (33.4 kcal mol^{-1} including zero-point and relativistic effects)[43] and with a recent experimental determination (35.5 ± 1.6 kcal mol^{-1}).[45] Energy decomposition analysis indicates that electrostatics dominate the Cu$^+-$CO interaction, but not to the extent found for Cu^{2+}. Thus, the Cu$^+-$CO bond is calculated to be 0.08 Å shorter than the Cu$^+-$OH$_2$ bond, and the Cu$^+-$CO and Cu$^+-$OH$_2$ bond energies are nearly equal. Cu$^+$ does not discriminate between H$_2$O and CO on the basis of their relative polarities. Again these same trends persist in the water model calculations.

The binding picture for Cu^0 is notably different from the above two cases. While matrix ESR experiments on CuCO have been interpreted in terms of a linear structure,[46,47] recent calculations indicate convincingly that the structure is actually bent.[48-50] The present calculations also find the bent structure to be more stable than the linear one, by 6 kcal mol^{-1}. One way this bending can be understood is in terms of an orbital mixing and electron density transfer from the singly occupied Cu 4s orbital to the CO 2π orbital, which is permitted by symmetry only for the bent structure. Thus, addition of CO to Cu^0 results in a partial oxidation of the Cu center, and the bonding can be described approximately as [Cu(I)$-$(C=O$^{\bullet-}$)]. The molecular orbital analysis (Figure 3) is consistent with this characterization: a singly occupied orbital is found several electronvolts higher in energy than the d manifold, containing an admixture of Cu 4s and CO π/σ orbital character. The transfer of electron density results in an electrostatic attraction between the two partially charged fragments, so that the Cu$-$CO bond energy is considerably greater than the Cu$-$OH$_2$ bond energy, where no such charge transfer mechanism is available. The bonding energy is calculated to be 13 kcal mol^{-1}, comparable to the earlier work,[48-50] but considerably less than in the Cu$^+$ and Cu^{2+} cases. Finally, because of the transfer of charge into the antibonding 2π orbital, the C$-$O bond is considerably lengthened compared to the free molecule.

In summary, then, CO binds to all three bare Cu species studied. For Cu$^+$ and Cu^{2+}, the binding is understandable in

TABLE 4: Selected Geometric Parameters and Mulliken Charges [LSDA] and Binding Energies [BP86] of $[Cu(H_2O)_xCO]^{n+}$ Complexes

	geometry[a]					Mulliken charge			binding energy[b]
	Cu–C	C–O	Cu–O	Cu–C–O	O_H–Cu–C	Cu	C	O_C	
$n = 2^c$									
$x = 0$	1.987	1.112		180.0		1.413	0.722	−0.135	−97.8
$x = 1$	1.939	1.111	1.894	177.4	163.5	1.141	0.624	−0.206	−185.5
$x = 2$	1.942	1.115	1.900	180.0	111.0	1.016	0.575	−0.235	−247.8
$x = 3$	1.881	1.117	1.992	180.0	108.7	0.862	0.556	−0.255	−279.9
$x = 4^d$	2.140	1.119	2.025	180.0	103.6	0.767	0.522	−0.290	−305.1
$x = 4^e$	1.872	1.121	2.110	180.0	109.2	0.748	0.549	−0.271	−299.0
$n = 1$									
$x = 0$	1.807	1.121		180.0		0.866	0.425	−0.291	−39.3
$x = 1$	1.784	1.124	1.872	180.0	180.0	0.694	0.446	−0.319	−81.7
$x = 2$	1.793	1.129	2.010	180.0	134.3	0.627	0.401	−0.345	−99.0
$x = 3$	1.793	1.133	2.078	180.0	123.4	0.561	0.401	−0.365	−113.0
$x = 4$	1.796	1.134	2.187	180.0	117.0	0.478	0.391	−0.377	−111.7
$n = 0$									
$x = 0$	1.869	1.151		140.7		0.102	0.318	−0.420	−12.6
$x = 1$	1.853	1.161	1.994	134.5	178.4	0.213	0.232	−0.465	−18.0
$x = 2$	1.851	1.174	2.147	133.2	136.2	0.229	0.180	−0.480	−20.4
$x = 3$	1.823	1.166	2.157	148.8	130.9	0.306	0.227	−0.482	−17.2
			2.128		125.3				
$x = 4$	1.787	1.147	2.249	164.2	103.7	0.467	0.352	−0.438	−14.7
			2.212		123.6				

[a] Distances in angstroms and angles in degrees. [b] Energy of reaction $Cu^{n+} + xH_2O + CO \rightarrow [Cu(H_2O)_xCO]^{n+}$, in kcal mol^{-1}. [c] Binding energy referenced to spherically averaged Cu^{2+} ion. [d] $(x^2 - y^2)^1$ state. [e] $(z^2)^1$ state.

terms of a primarily electrostatic interaction between CO and the Cu ion, with the more highly charged Cu^{2+} binding more strongly and more strongly perturbing the CO. For Cu^0, the binding is best understood in terms of a Cu 4s to CO 2π charge transfer and geometric reorganization of CO to accommodate the additional electron. In general, the binding energies increase with the Cu ion charge, but the *preference* for binding CO over H_2O decreases with increasing Cu charge. Thus, Cu^{2+} shows a strong preference for H_2O over CO, Cu^0 prefers CO over H_2O, and Cu^+ exhibits an approximately equal affinity for CO and H_2O. The CO bond length decreases with increasing Cu charge, suggesting that the CO vibrational frequencies should increase with increasing Cu charge. Such a trend has in fact been found for CO on silica-supported Cu, where distinct absorption peaks for CO bound to all three different oxidation states of Cu have been identified.[51]

Cu(H_2O)_xCO^{n+} Molecular and Electronic Structures. With this background, it is simple to understand the interaction of CO with Cu ions bound to framework oxygen in a zeolite. Again, the model we use is that of a Cu ion coordinated to one or more water molecules, but now with the addition of a single CO ligand inserted in the axial position. As in the homoleptic Cu–H_2O clusters above, symmetry constraints are imposed to provide a more realistic representation of the Cu–zeolite and Cu–CO interactions. Thus, the same caveats discussed above concerning optimization to local, symmetry-constrained energy extrema apply here.

The binding of CO to Cu complexes with one to four waters, i.e., $Cu(H_2O)_xCO^{n+}$ ($x = 1-4$, $n = 0-2$), has been investigated. For Cu^+ and Cu^{2+} with $x = 2-4$ water ligands, C_{xv} symmetry is assumed, with CO oriented along the principal axis of rotation and thus constrained to bind linearly to Cu. Test calculations indicate no tendency for CO to bend on these higher coordinate Cu sites. For $x = 1$ (i.e., Cu bound to a single water or bridge oxygen) both linear (C_{2v}, with a planar H_2O ligand) and bent (C_s, with a pyramidal water ligand) structures were considered, with Cu^+ preferring the former and Cu^{2+} the latter. A bent structure is preferred in all cases for Cu^0, as expected on the basis of the bare Cu results presented above. In our calculations, the CO is constrained to bend in the direction between adjacent

water ligands ($x > 1$) or between O–H vectors ($x = 1$), to yield C_s complexes. Possible computational difficulties associated with the lower symmetry bent configurations are discussed at length later on in the context of the $Cu(H_2O)_xNO^{n+}$ complexes, which exhibit a greater tendency for bending. Figure 1 contains representative sketches of the model geometries used here.

The important structural parameters for the $Cu(H_2O)_xCO^{n+}$ systems are summarized in Table 4. Addition of an axially coordinated CO ligand increases the pyramidalization at the Cu center and tends to increase the Cu–OH_2 bond distances. For instance, the Cu–O bond distances in $Cu(H_2O)_4^{2+}$ and Cu-$(H_2O)_2^+$ are 1.964 and 1.855 Å, respectively, and these increase to 2.025 and 2.010 Å upon addition of a CO. Again, these optimal distances are not unreasonable with respect to the dimensions of possible coordination sites within ZSM-5.

The binding of CO to the water-ligated Cu ions is similar to that for the bare ions. Thus, in all the $Cu(H_2O)_xCO^{2+}$ clusters considered, the optimal C–O bond length is less than that of the free molecule, reflecting the importance of electrostatics and σ donation in the Cu^{2+}–CO interaction. As H_2O ligands are added, the Cu^{2+} ion becomes more electron rich and less able to accept electron density from CO, with the result that the C–O bond length increases and the Cu–C bond length decreases.

The molecular orbital descriptions of the $Cu(H_2O)_xCO^{2+}$ complexes indicate strong mixing between d orbitals of the Cu^{2+} ion with both H_2O and CO orbitals, and the d orbital splitting patterns in these systems are complex. The molecular orbitals and Cu d orbital populations are consistent with the characterization of the systems as a Cu^{2+} ion plus weak donor ligands. For Cu^{2+}–CO clusters with up to three water ligands, the lowest energy state arises from singly occupying the Cu d_{z^2} orbital (taking the Cu–C axis as the z axis). With four water ligands, the $(x^2 - y^2)^1$ state drops slightly lower in energy than the $(z^2)^1$ one. While the difference in energy between these two states is small because of the primarily antibonding character of these two high-lying d orbitals, the Cu–C and Cu–O bond lengths differ considerably in the two states. The geometric and energetic results for both states are included in Table 4.

Similar trends are found in the $Cu(H_2O)_xCO^+$ systems. As the number of coordinated waters increases, the C–O bond

Cluster Models of Cu-Exchanged Zeolites

J. Phys. Chem., Vol. 100, No. 15, 1996 **6039**

length increases gradually, so that in $Cu(H_2O)_4CO^+$ the C—O bond length is slightly greater than that in the free molecule, suggesting at least some π back-bonding component to the Cu^+—CO bonding interaction. The Cu—C bond length is relatively invariant across the series. The molecular orbital description of the Cu^+—CO systems is considerably cleaner than in the Cu^{2+} case, because the primarily Cu d orbitals are well separated in energy from both the lower lying CO and H_2O orbitals, much as found in Figures 2 and 3. Thus, these systems can clearly be characterized as Cu^+ ions with d levels split by a combination of interactions with both CO and H_2O ligands.

Finally, the results for the $Cu(H_2O)_xCO^0$ clusters considered mirror those found for $CuCO^0$. The CO ligand binds in a bent fashion, and the C—O bond length is considerably increased over the free molecule. In the water-ligated clusters, as in $CuCO^0$, the bonding can best be described as a partial oxidation of the Cu atom to yield approximately a $[Cu(I)-CO^{\bullet-}]$ complex, with the unpaired electron localized in an essentially CO 2π orbital. The ability of the CO molecule to oxidize the Cu atom increases as the number of waters increases, as reflected in the increase in charge and decrease in s orbital population on the Cu center and the decrease in Cu—C bond length.

Thus, the geometric and electronic results for the $Cu(H_2O)_x-CO^{n+}$ clusters reinforce the conclusions drawn from the $CuCO^{n+}$ clusters: CO will bind on Cu^{2+}, Cu^+, and Cu^0 coordinated to additional water (or bridge oxygen) ligands. The CO bond lengths are modified by coordination of additional H_2O ligands to Cu, but the essential trends of decreasing CO bond length and increasing CO vibrational frequency with increasing Cu oxidation state hold true.

$Cu(H_2O)_xCO^{n+}$ Bond Energies. Table 4 also contains the binding energies for the Cu-CO complexes with respect to fragmentation into isolated Cu ions and H_2O and CO ligands. As found in the case of the homoleptic water complexes, the total binding energy decreases in magnitude from Cu^{2+} to Cu^+ to Cu^0. In all cases the complexes are bound with respect to the fragments. The Cu^0 results are notable in that the total binding energies are markedly larger than in the Cu^0—H_2O cases. The increase in binding results from the partial oxidation of the Cu^0 atom by the bound CO and the resultant electrostatic attraction between the partially cationic Cu and the dipolar H_2O and CO ligands.

The third column of Table 3 contains the binding energies for dissociation of the $Cu(H_2O)_xCO^{n+}$ clusters into $Cu(H_2O)_x^{n+}$ and CO. The effect of BSSE on the $Cu(H_2O)_4^+$—CO and $Cu(H_2O)_4^{2+}$—CO bond energies is estimated by the counterpoise method to be 2.2 and 2.5 kcal mol^{-1}, respectively. As with the water binding energies, this error is negligible for the present purposes, and BSSE is ignored in the results reported here.

A number of interesting trends are apparent from the CO binding energy results. As with the total binding energy, the CO binding energy is largest for Cu^{2+} and decreases for Cu^+ and Cu^0. In the first case, the $(H_2O)_xCu^{2+}$—CO bond energy is large for small x but falls off rapidly as x increases. The binding to Cu^{2+} is primarily electrostatic in character, and Cu^{2+} ion shows a strong preference for binding to the more highly polar H_2O ligands than to CO. As the coordination number of the ion increases and its ability to attract polar ligands decreases, the energetic preference for H_2O over CO decreases but is still present even at the highest coordination numbers considered here. As alluded to above, separation into $(H_2O)_xCu^+$ and CO^+ fragments also becomes thermodynamically unfavorable as x increases beyond 1. These results suggest that a Cu^{2+} ion will prefer to fill its coordination shell with H_2O (or bridge oxygen) ligands rather than with CO and that CO will not be able to

displace a H_2O (or bridge oxygen) ligand from Cu^{2+}. The presence of CO should not alter the preference of Cu^{2+} ions for high-coordination sites within a zeolite.

In contrast, Cu^+ is much less discriminating between H_2O and CO in its binding preferences. For lower coordination numbers, the Cu^+—CO and Cu^+—OH_2 binding energies are nearly the same. As the coordination number increases, both binding energies decrease, in particular in a discontinuous jump from two-coordinate $Cu(H_2O)^+$—L to three-coordinate $Cu(H_2O)_2^+$—L. Unlike Cu^{2+}, when Cu^+ is bound to two or more H_2O ligands, it has a slightly greater affinity for CO than it does for additional H_2O coordination. The results suggest that Cu^+ can more readily accommodate both CO and H_2O (or bridge oxygen) ligands in its coordination sphere and that CO should be able to displace H_2O (or bridge oxygen) from a zeolite-coordinated Cu^+ ion. This qualitative difference between Cu^{2+}—CO and Cu^+—CO binding is in accord with the common wisdom that Cu^+ will bind CO while Cu^{2+} will not. In fact, the results show that both Cu^+ and Cu^{2+} do bind CO, but that Cu^{2+} binds oxygen-containing ligands more strongly yet, and that these other ligands block addition of CO to the Cu^{2+} coordination sphere.

Finally, the Cu^0—CO bond energy is essentially invariant to the number of attached H_2O ligands and is consistently greater than the Cu^0—OH_2 bond energies in the homoleptic Cu^0-H_2O complexes. CO does bind to Cu^0. While the addition of H_2O ligands does not significantly alter the Cu^0—CO bond energy, the presence of the CO ligands does modify the Cu^0—OH_2 bond energies. For instance, the dissociation energy of $Cu(H_2O)_2$ from Table 2 is 0.3 kcal mol^{-1}, so that the two H_2O ligands are only weakly bound. In contrast, the energy to remove both H_2O ligands from $Cu(H_2O)_2CO$ can be calculated from Table 4 to be 7.9 kcal mol^{-1}. While not great, this difference does indicate that $CuCO^0$ has a greater affinity for H_2O ligands than does Cu^0 alone. Again, the increased binding is a result of the partial oxidation of Cu^0 brought about by coordination with CO and the electrostatic attraction between the partially cationic Cu center and the dipolar H_2O ligands that results. Addition of one or more H_2O ligands to $Cu(H_2O)_2CO$ is energetically unfavorable, however, and if such a system does exist, it will have very low coordination. These results suggest that, while monodispersed Cu^0 is not likely to be stable within a zeolite, monodispersed $CuCO^0$ may have a weak but favorable binding interaction with a small number of framework oxygens and may have some stability.

III. $Cu(H_2O)_xNO^{n+}$ Models. Understanding the interaction of NO with Cu sites in Cu—ZSM-5 is an important step toward understanding the activity of Cu—ZSM-5 in the decomposition and selective catalytic reduction reactions of NO. While the binding of a closed-shell CO ligand to a metal center is well-understood, NO, which differs from CO by the addition of an unpaired electron to the 2π shell, binds in a more complex fashion.[22] Traditionally, NO has been thought to interact with metal centers in two distinct modes. In the "linear" mode, the bonding is described in terms of a one-electron donation from NO to a metal center to form a formally NO^+ ligand, which is isoelectronic with and binds in a fashion analogous to CO. In the "bent" mode, NO accepts an electron from a metal center to form a formally NO^- ligand, which is isoelectronic with and binds in a fashion analogous to O_2.[52] The existence of both linear and bent NO coordination modes is well established,[22] but given the prominent covalent character of M—NO bonding, the assignment of formal metal oxidation states to M—NO complexes is now recognized to be ambiguous and potentially misleading.[22,53] Rather, Enemark and Feltham have proposed
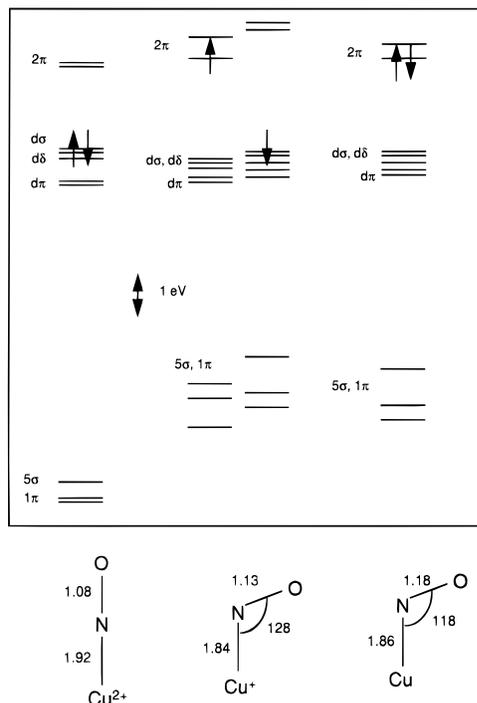
Figure 4. Molecular orbital diagrams for NO on bare Cu atom and ions. For ease of interpretation, the orbitals are shifted vertically so that the tops of the spin-up d orbital manifolds have the same energy.

a terminology in which the MNO moiety is treated as a whole and characterized by the sum of the number of metal d electrons plus one for each bound NO ligand.[53] Nonetheless, the use of the oxidation state terminology with respect to the Cu−NO interaction in Cu-ZSM-5 catalysts is widespread, and it is worthwhile to attempt to make a connection with this usage.

Discrete, well-characterized Cu−NO complexes are quite rare,[22,54] and a theoretical description of the Cu−NO interaction is available for only one model system.[54] We proceed here as in the CO case, by first examining the bonding in simple triatomic CuNO^{n+} complexes ($n = 0-2$) and then proceeding to the inclusion of H$_2$O ligands as models of coordination to zeolite bridge oxygens.

CuNO^{n+}. Table 4 contains LSDA geometry and BP86 energy results for CuNO^{n+} ($n = 0, 1, 2$), and Figure 4 contains molecular orbital diagrams for the three. Using the notation of Enemark and Feltham, these systems are described as {CuNO}^{10}, {CuNO}^{11}, and {CuNO}^{12}, respectively.[53] These electron counts are unusually large for nitrosyl complexes, and thus the bonding in the systems is expected to be somewhat unusual. Based on the qualitative discussion above, CuNO^{3+}, which is isoelectronic with CuCO^{2+} and can be described qualitatively as Cu^{2+}−N≡O$^+$ or {CuNO}^{9}, might also seem a molecule worth consideration. Electrostatic repulsion is very large in CuNO^{3+}, however, and the system is unbound with respect to Cu^{2+} and NO$^+$ at the LSDA level. We do not consider CuNO^{3+} in detail here, but do return to the question of the stability of the {CuNO}^{9} system later in the Results and Discussion.

The LSDA optimized bond length of free NO (1.154 Å) compares favorably with the experimental value (1.151 Å, Table 1). As with CO, NO binds to Cu^{2+} in a linear fashion, with the N−O bond length decreasing to 1.137 Å. CuNO^{2+} is isoelectronic with CuCO$^+$ and like the latter has a $^1\Sigma^+$ ground state. As shown in Figure 4, the electronic structure of CuNO^{2+} is characterized by distinct filled NO and Cu d manifolds, with the latter more than 2 eV lower in energy than the vacant NO 2π manifold. The d orbitals are split, with the dπ orbitals

stabilized below the other d orbitals. Thus, the bonding in CuNO^{2+} closely resembles the "linear" bonding model described above: an electron is transferred from NO to the Cu^{2+} (d^9) center, yielding a bonding situation that can be approximately represented as [Cu(I)−(N≡O$^+$)]. NO$^+$ is a stronger π acid than CO, and the NO 2π orbitals mix with and split off the Cu dπ pair. This same description of the {CuNO}^{10} system holds when H$_2$O ligands are added to the model.

The calculated Cu^{2+}−NO bond energy (-158 kcal mol^{-1}) is considerably larger than that of either Cu^{2+}−OH$_2$ or Cu^{2+}−CO, presumably because of the large covalent component in the interaction. The strong interaction suggests that Cu^{2+} within a zeolite may have a high affinity for NO. In fact, a relatively high-frequency feature in the infrared spectrum of "oxidized" Cu−ZSM-5 treated with NO has been assigned to NO bound on Cu^{2+},[55,56] and it has been argued that this adsorption process is a critical step in the NO decomposition reaction.[15] However, much like CuCO^{2+}, while the Cu^{2+}−NO bond is quite stable with respect to homolytic cleavage, it is unstable with respect to separation into Cu$^+$ and NO$^+$ fragments, by 106.5 kcal mol^{-1} at the BP86 level using the LDA geometries. Combined with the Cu^{2+}−NO bond energy, reduction of Cu^{2+} by NO is found to be exothermic by 264 kcal mol^{-1} in the gas phase, compared with the experimental result (based on gas-phase heats of formation at 0 K) of 254 kcal mol^{-1}.[57] While a very small (<1 kcal mol^{-1}) barrier to dissociation exists at the LDA level, optimization of the geometry at the BP86 level yields a barrierless separation into Cu$^+$ and NO$^+$ fragments. The instability of the Cu^{2+}−NO bond to heterolytic cleavage is unsurprising given the description of the bonding in terms of a charge transfer from NO to Cu^{2+} and the expected electrostatic repulsion of the two resultant cationic fragments. This instability is sharply reduced when H$_2$O ligands are added to the model, thus delocalizing the positive charge on the Cu$^+$ fragment, and it may disappear completely in more realistic models of zeolite systems. Nonetheless, the results suggest that NO may serve as a reductant for Cu^{2+} in zeolites, and this possibility should be recognized when considering possible mechanisms of NO decomposition and selective reduction.

CuNO$^+$ is isoelectronic with CuCO and, like the latter, adopts a bent geometry with a ^{2}A$'$ ground state.[58] The bent state is 8.9 kcal mol^{-1} more stable than a linearly constrained ($^2\Pi$) one at the BP86 level. The bending in the ^{2}A$'$ state is severe (LSDA ∠Cu−N−O = 127.5°), and the N−O bond length is just 0.02 Å less than that in the free molecule. A recent ab initio (coupled cluster with a small basis set) investigation of CuNO$^+$ finds the same qualitative geometric trends, although all bond lengths are larger and the bending is smaller.[58] As shown in Figure 4, the electronic structure of CuNO$^+$ is derived from that of CuNO^{2+} by the addition of a single electron into the NO 2π manifold. As with CuCO, rehybridization of the 2π orbital with the Cu 4s provides the driving force for bending of CuNO$^+$. The bonding situation can be conveniently represented as [Cu(I)−^{2}(N=O•)], where the superscript 2 (doublet) notation is used to emphasize that the unpaired electron is largely localized on NO, in this case in an in-plane hybrid orbital. If CuNO$^+$ is imagined as arising from the interaction of a Cu$^+$ cation with NO, the Cu center is neither oxidized nor reduced by the NO ligand, and the bonding is best described as a simple dative electron pair donation from NO to the Cu center, supplemented by back-donation from Cu to the vacant orbital of NO 2π origin. This same description has been used for the bonding of an amine-coordinated {CuNO}^{11} system,[54] and as we will show it is also appropriate for the H$_2$O-ligated models. The geometric and electronic structure results suggest that NO

Cluster Models of Cu-Exchanged Zeolites

J. Phys. Chem., Vol. 100, No. 15, 1996 **6041**

adsorbed on Cu^+ within a zeolite should have a lower frequency stretch than that found for Cu^{2+}. Such a correlation has been observed.[55]

The Cu^+-NO bond energy is 33 kcal mol^{-1} at the BP86 level, slightly larger than that found in the earlier ab initio work.[58] This binding energy is much less than that found for $Cu^{2+}-NO$, but unlike $CuNO^{2+}$, $CuNO^+$ is stable to separation into fragments such as Cu and NO^+. The Cu^+-NO bond energy is also slightly less (by 6 kcal mol^{-1}) than that found for Cu^+-OH_2 and Cu^+-CO, but the difference between these three is not great. Unlike Cu^{2+}, Cu^+ does not strongly discriminate between H_2O, CO, and NO, suggesting that the nature of the interaction between Cu^+ and the three ligands is similar.

$CuNO^0$ is the only member of the $CuNO^{n+}$ series that has been directly observed experimentally, in an Ar matrix isolation experiment.[59] $CuNO^0$ adopts a bent geometry and has a $^1A'$ ground state, but with a $^3A''$ state only 2.0 kcal mol^{-1} higher in energy at the BP86 level. Linearly constrained $^3\Sigma^-$ and $^3\Pi$ states are both approximately 18 kcal mol^{-1} higher in energy. The bending in the $^1A'$ ground state (LDA $\angle Cu-N-O = 118.4°$) is even more severe than that in $CuNO^+$, and the N–O bond length is 0.02 Å greater than in the free molecule. Again, the same general geometric trends have been found in the ab initio calculations, with only a slightly larger (5.5 kcal mol^{-1}) singlet–triplet splitting.[58] The bond length variation is also consistent with the available spectroscopic information.[59] From Figure 4, the electronic structure of $CuNO^0$ can be qualitatively derived from that of $CuNO^+$ by the addition of a second electron into the NO 2π derived orbitals, either spin-paired ($^1A'$) in an in-plane, N-centered orbital derived from the NO 2π set or spin-parallel ($^3A''$) in the orthogonal in-plane and out-of-plane NO 2π-derived orbitals. Thus, the bonding situation for $\{CuNO\}^{12}$ can be represented approximately as $[Cu(I)-^{1,3}(N=O^-)]$, with the unpaired electron density in the triplet case largely localized on NO. If $CuNO^0$ is imagined as being formed from an isolated Cu atom and an NO ligand, the Cu atom is oxidized by one electron by NO, and the $CuNO^0$ bonding resembles the "bent" model described above. The highest lying orbitals of CuNO are not pure ligand in character, as bending introduces mixing between the NO 2π and the Cu 4s orbitals, and the one-electron transfer model is of course only an approximate, but useful, description.

The charge transfer bonding model suggests some electrostatic contribution to the bonding in CuNO. The calculated Cu–NO bond energy is 24 kcal mol^{-1} at the BP86 level, again somewhat larger than the earlier ab initio work.[58] The bond energy is only 9 kcal mol^{-1} less than that found for Cu^+-NO and is greater by 11 and 21 kcal mol^{-1} than that found for Cu–CO and $Cu-OH_2$, respectively. Thus, the Cu–NO bond is predicted to be fairly robust, as the limited experimental results suggest.[59]

In summary, then, NO is found to bind to Cu in $CuNO^{2+}$, $CuNO^+$, and $CuNO^0$. In each case, the binding is best understood in terms of a Cu(I) species interacting with either NO^+, NO radical, or NO^- (singlet or triplet), respectively. Thus, definition of a Cu oxidation state in a nitrosyl complex is ambiguous, and it is preferable to identify these as $\{CuNO\}^{10}$, $\{CuNO\}^{11}$, and $\{CuNO\}^{12}$. The N–O bond lengths increase across the series as electrons are added into the formally NO 2π antibonding orbital, and the N–O vibrational frequencies are expected to decrease commensurately. All three species are bound with respect to loss of NO, with $CuNO^{2+}$ having the largest binding energy and $CuNO^+$ and $CuNO^0$ having much less. Further, both Cu^{2+} and Cu^0 have a strong preference for binding NO over H_2O or CO, while Cu^+ shows almost an equal affinity for CO, NO, and H_2O. Finally, while $CuNO^{2+}$ is

strongly bound with respect to loss of NO, it is unbound with respect to loss of NO^+, and reduction of Cu^{2+} by NO is a highly exothermic process. The same qualitative behavior is found when H_2O ligands are included in the model, as we now show.

$Cu(H_2O)_xNO^{n+}$ Molecular and Electronic Structures. The models of NO coordination within Cu-exchanged zeolites are analogous to those used above in the CO case: bridge oxygens are modeled by water ligands arranged approximately equatorially about Cu, with the NO ligand added axially. The model systems include $Cu(H_2O)_xNO^{n+}$ ($x = 1-4$, $n = 0-2$). In virtually all cases, both linear (C_{xv}, $x > 1$) and bent (C_s) coordinations of the NO ligand have been examined. The lower symmetry of the bent systems causes two problems in calculating structures and relative energies that need to be addressed. First, in most of the $Cu(H_2O)_x^{n+}$ and $Cu(H_2O)_xCO^{n+}$ model compounds already discussed, symmetry was used to constrain the system to a "zeolite-like" C_{xv} coordination geometry, i.e., pseudoplanar $[Cu(H_2O)_x^{n+}]$ or pseudopyramidal $[Cu(H_2O)_x-CO^{n+}]$. In bent systems, symmetry constraints alone cannot ensure optimization to a pseudopyramidal structure, and care must be taken during the optimization process to locate a local minimum that is a reasonable approximation to the desired model geometry. Second, an unbiased comparison of the energies of optimized linear and bent systems is difficult, because the latter may be artificially stabilized relative to the former by the additional relaxation of the H_2O ligands permitted in the reduced symmetry. Thus, in all cases examined for $Cu(H_2O)_xNO^{n+}$, a bent, lower symmetry structure can be found that is lower in energy than the linear, higher symmetry counterpart, but whether the lower energy is truly a consequence of allowing the NO to bend or is simply an artifact of the model is not always clear.

Because of these additional complications, we construct the $Cu(H_2O)_xNO^{n+}$ model systems as follows. For the Cu^0 and Cu^+ cases, where the bare Cu results clearly indicate the tendency for NO to bend, we report results for both linear and bent NO coordination on the water models. The linear and bent systems tend to be energetically and structurally similar, and both coordination modes may be important for these electron counts. The geometries chosen for bent NO are the same as those discussed for CO: NO is constrained to bend in the direction "between" the Cu–O bond vectors (for $x > 1$) or between the O–H vectors (for $x = 1$), under the constraint of C_s symmetry. For the Cu^{2+} case, the choice of model geometries to report is less clear. Again, both linear and bent structures can be obtained. The largest energetic difference between linear and bent geometries occurs with $Cu(H_2O)_4NO^{2+}$, where the fully relaxed bent structure is more stable than the linear one by 11 kcal mol^{-1} at the LDA level. However, constraining the $Cu(H_2O)_4$ structure to the C_{4v} geometry while allowing the NO to bend reduces the difference to only 3.5 kcal mol^{-1}. In the lower coordinate structures, the bent geometry is similarly preferred over the linear one, but bending is accompanied by large relaxations of the $Cu(H_2O)_x$ structure. Because the direct contribution of NO bending to the stabilization is difficult to unravel, and because the energetic differences are too small to bear on the qualitative discussion, we only report results for linearly coordinated NO on Cu^{2+}. All these model geometries are presented in Figure 1.

The important structural parameters for the $Cu(H_2O)_xNO^{n+}$ complexes are summarized in Table 5. The general features of NO coordination are similar to CO coordination: addition of an NO ligand increases both the pyramidalization angle at the Cu center and the Cu–O bond distances, irrespective of the overall cluster charge. In the Cu^+ and Cu^0 complexes, only

TABLE 5: Selected Geometric Parameters and Mulliken Charges [LSDA] and Binding Energies [BP86] of $[Cu(H_2O)_xNO]^{n+}$ Complexes

	state	geometry[a]					Mulliken charge			binding energy[b]
		Cu−N	N−O	Cu−O	Cu−N−O	O_H−Cu−N	Cu	N	O_N	
$n = 2$[c]										
$x = 0$	$^1\Sigma^+$	1.917	1.079		180.0		1.275	0.611	0.114	−158.0
$x = 1$	$^1A_1$	1.755	1.088	1.837	180.0	180.0	1.141	0.505	0.068	−226.0
$x = 2$	$^1A_1$	1.781	1.095	1.939	180.0	131.3	1.050	0.461	0.016	−270.9
$x = 3$	$^1A_1$	1.740	1.102	1.998	180.0	122.3	0.947	0.394	−0.029	−304.6
$x = 4$	$^1A_1$	1.756	1.103	2.081	180.0	113.9	0.839	0.409	−0.041	−316.2
$n = 1$										
$x = 0$	$^2\Pi$	1.795	1.143		180.0		0.960	0.206	−0.166	−24.6
$x = 1$	$^2B_2$	1.737	1.147	1.852	180.0	180.0	0.816	0.194	−0.195	−71.2
$x = 2$	$^2B_1$	1.744	1.154	1.991	180.0	132.8	0.748	0.153	−0.237	−92.8
$x = 3$	^2E	1.784	1.159	2.077	180.0	122.3	0.631	0.179	−0.269	−104.2
$x = 4$	^2E	1.778	1.161	2.148	180.0	114.1	0.597	0.163	−0.286	−105.6
$x = 0$	$^2A'$	1.844	1.137		127.5		0.865	0.252	−0.117	−33.4
$x = 1$	$^2A'$	1.778	1.150	1.885	135.5	176.1	0.784	0.205	−0.172	−73.6
$x = 2$	$^2A'$	1.792	1.158	1.997	134.7	133.1	0.731	0.153	−0.219	−94.7
$x = 3$	$^2A'$	1.792	1.162	2.056	142.5	119.8	0.657	0.157	−0.256	−105.5
				2.041		121.6				
$x = 4$	$^2A'$	1.836	1.167	2.185	127.6	111.2	0.586	0.156	−0.262	−110.6
				2.158		116.4				
$n = 0$										
$x = 0$	$^3\Sigma^-$	1.721	1.213		180.0		0.518	−0.104	−0.414	−6.1
$x = 1$	$^3A_2$	1.719	1.215	1.881	180.0	180.0	0.397	−0.090	−0.442	−32.3
$x = 2$	$^3A_2$	1.730	1.222	2.087	180.0	137.9	0.367	−0.097	−0.467	−35.1
$x = 3$	$^3A_1$	1.753	1.222	2.199	180.0	128.5	0.315	−0.074	−0.486	−39.2
$x = 4$	$^3A_1$	1.783	1.225	2.282	180.0	111.4	0.312	−0.080	−0.476	−36.0
$x = 0$	$^1A'$	1.858	1.177		118.4		0.202	0.078	−0.280	−25.9
$x = 1$	$^3A''$	1.770	1.217	1.917	132.9	177.5	0.398	−0.082	−0.404	−38.3
$x = 2$	$^3A''$	1.786	1.226	2.101	132.5	136.7	0.398	−0.106	−0.436	−38.3
$x = 3$	$^3A''$	1.789	1.228	2.178	134.9	130.6	0.378	−0.092	−0.451	−38.5
				2.202		130.4				
$x = 4$	$^3A''$	1.811	1.228	2.327	136.0	124.5	0.336	−0.080	−0.454	−39.9
				2.324		115.2				

[a] Distances in angstroms and angles in degrees. [b] Energy of reaction $[Cu(H_2O)_xNO]^{n+} \rightarrow Cu^{n+} + xH_2O + NO$, in kcal mol^{-1}. [c] Binding energy referenced to spherically averaged Cu^{2+} ion.

minor structural relaxation is observed upon allowing NO to bend. Again, the structural results are not inconsistent with the expected dimensions of coordination sites within zeolites, such as ZSM-5.

The bare CuNO^{n+} complexes provide a sound basis for understanding the binding of NO to oxygen-ligated Cu ions. In all the Cu^{2+}−NO ({CuNO}^{10}) clusters the N−O bond length is significantly diminished over that of the free molecule. As the number of attached H$_2$O ligands is increased and the Cu center becomes more electron rich, the N−O bond length increases, but only slightly. The electronic structure of these clusters is complex because of the strong mixing between the energetically similar Cu d levels and the O levels from H$_2$O. The essential features of bare CuNO^{2+} are not lost, however. The NO 5σ and 1π levels can be identified and are lower in energy and well separated from the Cu d and H$_2$O manifolds, while the vacant NO 2π orbitals are 1 eV or more higher in energy than the top of the Cu/H$_2$O manifold. The characterization of these {CuNO}^{10} systems is thus the same as in the water-free case: the Cu center is approximately reduced by one electron by the NO ligand, and the resultant bonding situation can be represented as $[(H_2O)_xCu(I)-(N\equiv O^+)]$. The large contribution of covalence, particularly in the Cu dπ−NO$^+$ 2π interaction, is confirmed by a bond energy decomposition analysis.

As in bare CuNO^{2+}, the Cu(H$_2$O)$_x$NO^{2+} clusters are unstable towards dissociation into Cu(H$_2$O)$_x^+$ and NO$^+$, because of the electrostatic repulsion between the two fragments. The addition of H$_2$O ligands both decreases the dissociation energy and increases the barrier to separation, at both the LDA and BP86 levels of calculation. Stronger donor or anionic ligands, such

as framework oxygen near Al sites within a zeolite lattice or extralattice OH$^-$, would likely stabilize these {CuNO}^{10} systems even further. Thus, we expect the {CuNO}^{10} systems to be kinetically robust, but to at least have the potential for thermodynamic instability. As noted above, the energy of the Cu(H$_2$O)$_x$NO^{2+} clusters can be lowered by allowing the NO ligands to bend. Along with the additional relaxation of the Cu(H$_2$O)$_x$ fragment that bending permits, it also facilitates structural relaxation toward the separated ions, characterized in some cases by large increases in the Cu−N bond distance. We thus believe this bending of NO to be an artifact of the water model and not a real characteristic of the {CuNO}^{10} system.

The Cu(H$_2$O)$_x$NO$^+$ results are similarly understood in terms of those for CuNO$^+$. Results for both linearly and bent coordination are shown in Table 5. The N−O bond lengths in the Cu$^+$−NO ({CuNO}^{11}) clusters are comparable with to slightly longer than that in the free NO molecule and do not vary greatly upon bending. While rather dramatic bending of the NO ligand is energetically preferred in every case, the difference in energy between linear and bent structures is much less than in bare CuNO$^+$, and the structural relaxation upon bending is also relatively minor. The one structurally characterized {CuNO}^{11} complex has a Cu−N−O bond angle of 163.4°,[54] intermediate between the optimized bent and linear NO results here. It would appear that in the ligated {CuNO}^{11} systems the Cu−N−O bending potential is soft and that the bond angle is likely determined by factors external to the CuNO unit.

In moving from the Cu^{2+}−NO clusters to the Cu$^+$−NO ones, an electron is added to the orbitals derived from the NO 2π

Cluster Models of Cu-Exchanged Zeolites

J. Phys. Chem., Vol. 100, No. 15, 1996 **6043**

manifold. In the three- and four-H_2O cases, then, the linear NO geometries are of ^2E symmetry and are Jahn−Teller active, which likely contributes to the bending of the NO. Upon bending of the NO, the unpaired electron becomes localized in the in-plane orbital derived from the NO 2π manifold, and the ground states of the bent structures are thus all of $^2A'$ symmetry. Population analysis confirms that the majority of the spin density resides on the nitrogen center, with the remainder primarily on the NO oxygen. The bonding picture thus described is identical to that obtained for bare $CuNO^+$, and can be represented approximately as $[(H_2O)_xCu(I)−^2(N{=}O^\bullet)]$, so that formally the Cu^+ center is neither oxidized nor reduced by the addition of NO. Bond energy analysis for $Cu(H_2O)_2{}^+−NO$ indicates that the interaction is largely covalent, with a particularly large contribution to the bonding derived from the Cu $d\pi$−NO π interaction. The importance of covalence in $\{CuNO\}^{11}$ bonding has also been emphasized in the earlier ab initio work.[54]

Unlike the above two cases, the $Cu(H_2O)_xNO^0$ clusters exhibit some important qualitative differences from bare $CuNO^0$. Like bare $CuNO^0$, the N−O bond lengths in the $Cu^0−NO$ ($\{CuNO\}^{12}$) clusters are considerably longer than that found in the free NO molecule, and the bond length increases with the addition of H_2O ligands, as the Cu center becomes more electron rich and a better electron donor. Again, both linear and bent NO coordination geometries for $Cu(H_2O)_xNO^0$ have been investigated, and while the Cu−N−O bending is very pronounced in the latter, the energetic difference between linear and bent structures is almost negligibly small, as is the difference in N−O bond length. This indifference to bending is in sharp contrast to bare $CuNO^0$, where the bending is strongly preferred, but is similar to the results obtained for the $Cu^+−NO$ clusters. Ligation apparently results in a decrease in the Cu−N−O bending potential for $Cu^0−NO$ complexes, and while no structurally characterized $\{CuNO\}^{12}$ complexes are known, it is likely that any bending of the NO ligand in such systems will again result from factors external to the CuNO unit. The Cu−N bond lengths are also similar to those found in the $Cu^+−NO$ clusters, and as in those clusters, the Cu−N bond lengths tend to increase with bending of the N−O ligand.

The similarities between the $Cu^+−NO$ and $Cu^0−NO$ systems are not coincidental. The $Cu^0−NO$ complexes are obtained from the $Cu^+−NO$ ones by the addition of a second electron into the pair of orbitals derived from the NO 2π set. In the linear case, where the orbitals are degenerate [CuNO, $Cu(H_2O)_3$-NO, and $Cu(H_2O)_4NO$] or nearly degenerate [$Cu(H_2O)NO$ and $Cu(H_2O)_2NO$] the electrons combine spin-aligned, and triplet ground states are obtained. In bare $CuNO^0$, bending is facilitated by the mixing between the NO 2π orbitals and the Cu 4s orbital, leading to a ground state singlet system. Additional H_2O ligands are also able to interact with the Cu 4s orbital, however, making it less available for mixing with the NO 2π orbitals. The driving force for bending is diminished, as is the driving force for pairing the two electrons upon bending. Thus, unlike bare $CuNO^0$, the ground states of all the bent $Cu^0−NO$ clusters are $^3A''$, with the two unpaired electrons localized in the orthogonal orbitals derived from the NO 2π set. Mulliken population analysis confirms that the majority of the spin density resides on the N and O centers. Because the second electron is largely nonbonding with respect to the Cu−N bond and the Cu−N−O bend, one expects and finds the structural results for the $Cu^0−NO$ systems to be similar to those for the $Cu^+−NO$ ones.

We return now to the question of the existence and stability of the $\{CuNO\}^9$ system. Again, the unligated member of this category, $CuNO^{3+}$, is unstable to dissociation into Cu^{2+} and

NO^+ because of the strong electrostatic repulsion in the system. Similarly, $Cu(H_2O)_4NO^{3+}$ is unstable and separates without barrier at the LSDA level into $Cu(H_2O)_4{}^{2+}$ and NO^+ fragments, again because of the strong electrostatic repulsion present. These results do not exclude the possibility of the existence of lesser charged $\{CuNO\}^9$ complexes, however. To explore this question further, several calculations were performed on the neutral system $Cu(OH)_3NO$, which by standard electron counting rules would be characterized as $\{CuNO\}^9$.[53] The complex examined has C_{3v} symmetry and a ^2E ground state. While $Cu(OH)_3NO$ is stable against dissociation into molecular or ionic fragments, it has an electron affinity at the LSDA level of over 110 kcal mol^{-1}. Many of the cationic systems considered in this work have similarly large or larger calculated electron affinities, but this result is remarkable for a neutral complex. It suggests that $Cu(OH)_3NO$ strongly desires to become $Cu(OH)_3NO^-$, or $\{CuNO\}^{10}$. Further, molecular orbital analysis indicates that the electronic structure can best be described as $[(HO^{2/3-})_3Cu(I)−(N{\equiv}O^+)]$; that is, while the system is formally $\{CuNO\}^9$, it very much looks like a $\{CuNO\}^{10}$ system with a hole in the manifold of formally OH$^-$ orbitals. The few calculations performed here clearly do not serve to fully characterize the $\{CuNO\}^9$ system, particularly as it may occur within a zeolite. The results do suggest, however, that $\{CuNO\}^9$ is not a particularly stable electronic configuration and that the three most robust electronic configurations for NO bound on Cu are $\{CuNO\}^{10}$, $\{CuNO\}^{11}$, and $\{CuNO\}^{12}$. These three structures likely provide the best characterization of NO bound to Cu within ZSM-5.

In summary, then, the $Cu(H_2O)_xNO^{n+}$ structural and electronic results are consistent with three types of Cu-NO linkages within zeolites. As in the bare Cu ion case, these can be characterized as $\{CuNO\}^{10}$, $\{CuNO\}^{11}$, and $\{CuNO\}^{12}$, or perhaps more descriptively, as $[Cu(I)−(N{\equiv}O^+)]$, $[Cu(I)−^2(N{=}O^\bullet)]$, and $[Cu(I)−^{1,3}(N{=}O^-)]$, respectively. Again, because of the high degree of covalency in the Cu−NO interaction, formal oxidation states cannot readily be assigned to the Cu centers alone, but rather the CuNO system must be taken as a unit that overall can assume three different "oxidation states". As one moves across the series of increasing electron count, unpaired electron density builds up primarily on the nitrogen center, suggesting that coordination to Cu may enhance the reactivity of NO. Structurally, the N−O bond lengths increase, and vibrational frequencies presumably decrease, as the electron count increases. Both linear and bent coordination geometries have been investigated, and the energetic differences between the two are smaller, so that the coordination geometry will likely differ from system to system with the same overall electron count.

Cu(H_2O)_xNO^{n+} Bond Energies. The last column of Table 5 contains the energy for dissociation of the $Cu(H_2O)_xNO^{n+}$ clusters into Cu^{n+}, H_2O, and NO fragments. The general trends are not surprising: all the systems studied are stable with respect to dissociation, and the total binding energy decreases with decreasing net positive charge on the systems.

The binding energies from Tables 2 and 5 are used to calculate the $Cu(H_2O)_x{}^{n+}−NO$ bond energies, which are reported in the last column of Table 3. In the $n = 0$ and $n = 1$ cases, where both linear and bent NO coordination modes have been examined, the Cu−NO bond energy is for the lowest energy (most stable) structure found. As above, the effect of BSSE on the bond energies has been examined. For $Cu(H_2O)_2{}^+−NO$ and $Cu(H_2O)_4{}^{2+}−NO$, the BSSE contribution to the binding energy is estimated using the counterpoise method to be 3.4 and 4.1 kcal mol^{-1}, respectively. While larger than the errors

found for either individual $Cu-OH_2$ or $Cu-CO$ bond energies, for the present qualitative purposes the errors are negligible and can be ignored.

NO is strongly bound in all of the Cu^{2+} ({CuNO}[10]) clusters, although as with the H_2O and CO binding energies, the NO binding energy falls off rapidly with increasing coordination number. NO binds to Cu^{2+} by donation of its lone 2π electron, and as the degree of H_2O coordination increases and the ability of Cu^{2+} to accept additional electron density decreases, the $Cu^{2+}-NO$ binding energy decreases. NO has a commensurate effect on the $(NO)(H_2O)_{x-2}Cu^{2+}-OH_2$ bond energy, decreasing it with respect to that of the corresponding $(H_2O)_{x-1}Cu^{2+}-OH_2$ bond energy by approximately 10 kcal mol^{-1}. Because of the large contribution of covalence, the $Cu^{2+}-NO$ bond energy is greater than the $Cu^{2+}-CO$ bond energy and greater than or equal to the $Cu^{2+}-OH_2$ bond energy in all the systems considered, i.e., $Cu^{2+}-NO \geq Cu^{2+}-OH_2 > Cu^{2+}-CO$. On the basis of the relative bond energies, we argued earlier that CO should not be able to displace a H_2O (or presumably bridge oxygen) ligand from the coordination shell of a Cu^{2+} ion. By the same reasoning, because NO binds more strongly to Cu^{2+} than does H_2O, NO is able to displace H_2O (or bridge oxygen) ligands from the Cu^{2+} coordination sphere. The results indicate that oxygen-coordinated Cu^{2+} should have a high affinity for NO, consistent with the affinity for NO observed for cupric oxide[60] and for "oxidized" Cu–ZSM-5.[17,55]

As noted above, all of the CuNO^{2+} systems are unstable to separation into Cu^+ and NO$^+$ fragments. From the binding energy results we calculate dissociation to be exothermic by 77, 72, 50, and 41 kcal mol^{-1} for the systems with one to four added H_2O ligands, respectively. The instability to dissociation does diminish with increasing coordination, and in systems in which the overall charge is neutralized by other ligands or framework Al, the instability may disappear altogether. Further investigation of this point is clearly necessary. However, both the electronic structure and energetic results do suggest that NO will both bind to and act as a reductant of Cu^{2+} coordinated to oxygen-containing ligands.

NO is much less strongly bound in the Cu^+ ({CuNO}[11]) systems than in the Cu^{2+} ones. The same binding energy trend is found for NO as for CO and H_2O: the Cu^+-NO bond energy is essentially the same in the zero and one H_2O systems and decreases by approximately 20 kcal mol^{-1} in the higher coordinate complexes. The Cu^+-OH_2 bond energy is slightly larger than the Cu^+-NO bond energy for low coordination numbers, but is slightly smaller for higher coordination, while the Cu^+-CO bond energy is slightly larger than either at any level of coordination. In all three cases the binding primarily arises from a dative interaction between the Cu center and the ligands. For low (1 or 2) coordination, the better donor ligands are preferentially bound. For higher coordination (3 or more), the stronger donor ligands become less preferable to the weaker donor, stronger π-acceptor ligands. The energetic differences are not large, however, and at the level of reliability of the present study we have $Cu^+-OH_2 \approx Cu^+-CO \approx Cu^+-NO$. In zeolites it is likely that Cu^+ is not able to discriminate strongly between CO, NO, or H_2O (or bridge oxygen) coordination and that the three should be readily exchanged within the Cu^+ coordination shell.

NO is bound as or more strongly in the Cu^0 ({CuNO}[12]) complexes than in the Cu^+-NO ones. Further, unlike the Cu^{2+} and Cu^+ cases, the Cu–NO bond strength is actually found to increase slightly as H_2O ligands are added and the Cu center becomes more readily oxidized. A direct comparison of these three is somewhat misleading, however. From the last column

of Table 5, the total binding energy of the bent $Cu(H_2O)_xNO$ systems is essentially invariant for $x \geq 1$, indicating that H_2O ligands beyond the first are essentially unbound. As with Cu^0-CO complexes, Cu^0-NO complexes only exist for very low coordination numbers. NO does bind more strongly to Cu^0 than does CO or H_2O, and in general $Cu^0-NO > Cu^0-CO > Cu^0-OH_2$. The results suggest that Cu^0-NO could exist as a species weakly coordinated to a zeolite lattice. It is highly unlikely that such a system would form within a zeolite from the combination of a zeolite-coordinated Cu^0 atom with a free NO molecule. It is conceivable, however, that a {CuNO}[12] structure could exist as an intermediate, perhaps formed by the reduction of a {CuNO}[11] (Cu^+-NO) structure, and then participate in some further chemistry.

IV. Extension beyond the H_2O Model. The issue of how well the water ligand model reproduces the actual properties of bound Cu ions and Cu–CO and Cu–NO complexes in zeolites is the subject of ongoing investigations.[61] Legitimate concerns exist about the adequacy of the cluster sizes considered and the use of charged clusters, rather than explicit countercharges, to vary the Cu oxidation state. To address these questions, we have performed calculations on larger clusters containing more realistic models of Cu ions coordinated to zeolite frameworks. The details of these comparisons will be presented separately,[61] but as support for the work reported here, we provide here a brief summary of the results.

Results have been obtained for two larger cluster models at the opposite extremes of oxygen coordination number. The first is for 1-fold coordinated Cu, with the single H_2O ligand in the water model replaced by an $X_3TOT'X_3$ zeolite bridge, with T, T' = Si or Al and X = H or OH. The second is for 4-fold coordinated Cu, with the four H_2O ligands replaced by an elongated $(OSiX_2)_4(OTX_2)_2$ 6-fold ring, such as that present in ZSM-5. In both cases, a number of symmetry-preserving, constrained optimizations have been performed for purely siliceous charged clusters, with or without additional CO or NO ligands, as well as for neutral clusters containing one or two aluminums. Comparisons of the results of these more realistic models to those of the corresponding water ligand model yield remarkably similar qualitative conclusions in the two cases.

The water ligand model predictions for Cu^0 and Cu^+ are extremely robust. Bonding geometries, electronic structures, and CO and NO binding energies are little changed (<5 kcal mol^{-1}) in going to any of the corresponding larger H- or OH-terminated models. The binding energies of Cu^+ to "framework oxygen" do increase significantly (~100 kcal mol^{-1}) in the larger models if neutral, Al-containing clusters are used instead of charged, siliceous clusters. This result is not surprising, because the explicit inclusion of the compensating negative framework charge increases the electrostatic attraction of the ion. The presence of aluminum, however, has little effect on the subsequent interactions of bound Cu^+ ions with CO or NO. In comparing the water ligand and larger models, care was taken to constrain the geometries of the larger models to maintain the desired Cu^+ coordination. If these constraints are removed, the larger "1-fold" structures tend to distort, especially if Al is present, to allow the copper to coordinate to additional oxygen or peripheral hydrogen atoms. Such distorted structures are not directly comparable to any water ligand results, but they do illustrate again the strong preference of Cu^+ for at least 2-fold coordination.

Some differences between the water ligand and larger model results are observed in the case of Cu^{2+}. As found above in its interaction with NO, Cu^{2+} has a strong tendency to oxidize ligands. Such behavior is also found in the interaction of Cu^{2+}

Cluster Models of Cu-Exchanged Zeolites

J. Phys. Chem., Vol. 100, No. 15, 1996 **6045**

with the larger single bridge oxygen models. For instance, Cu^{2+} does bind strongly to $O(SiH_3)_2$ or $O(AlH_3)_2^{2-}$, but in both cases the Cu center oxidizes the ligand and thus appears as Cu(I), with the remaining charge and unpaired spin density delocalized to the periphery of the cluster. The oxidation of these larger, T-atom-containing clusters can be understood in terms of the wider energy distribution of the cluster-derived orbitals in combination with the weak ligand field splitting of the Cu d orbitals, which results in a strong overlap between and charge transfer from the ligand levels to the Cu d shell. Calculated CO binding energies in these larger single bridge oxygen models, in fact, lie very close to the $n = 1$ (not $n = 2$!) results in the corresponding water ligand model.

This discrepancy does not diminish the value of the water model for Cu^{2+}, however. A single bridge oxygen coordination site, be it represented by H_2O or $O[Si(OH)_3]_2^{2-}$, is in fact a very poor model for Cu^{2+} exchanged into ZSM-5. As we have found here, and as is well-known from experiment, Cu^{2+} has a strong tendancy toward higher coordination numbers and in ZSM-5 is likely bound to at least four lattice oxygens. In describing the chemistry of Cu^{2+}, it is far more important to properly represent the overall coordination geometry of the metal center than it is to develop an accurate representation of a single lattice oxygen. Thus, when more realistic "zeolite-like" Cu^{2+} coordination sites are employed and properly relaxed, such as the 4-fold site within an $(OSiX_2)_4(OTX_2)_2$ 6-fold ring, the discrepancies between the water and more "realistic" models disappear: the electronic structure at the metal center is unchanged, as is the binding of CO or NO on the Cu site. For the coordination geometries likely to be important within ZSM-5, then, the Cu^{2+}–water model is robust.

Thus, the comparisons between the water model results and the larger zeolite models do support the use of the simpler model. A caveat about the water ligand model (or the more elaborate models) bears repeating, however. While the idealized coordination geometries assumed here are useful for identifying trends, the actual Cu binding sites in any particular zeolite will be strongly influenced by additional factors such as the location of aluminum and possible restrictions imposed by the framework topology and geometry. Cu^{2+}, for example, is known to occupy what we would call 3-fold sites at the center of highly symmetric 6-fold rings in zeolite A and faujasite,[7] but no likely 3-fold sites are apparent in ZSM-5. The additional electrostatic interactions and symmetry breaking caused by aluminum can also make a Cu ion prefer a lower coordination site than it might otherwise and alter the relative preferences of Cu^{2+}, Cu^+, and Cu^0 for framework oxygen, CO, and NO.

Clearly, a more realistic cluster model is preferable to one based exclusively on water ligands whenever the location of the extralattice cation of interest is well-established (e.g., a Brønsted acid site). However, when such information is not available, as in Cu–ZSM-5, the use of a too detailed–and potentially incorrect–model introduces strong biases into the results that can lead to incorrect conclusions. In such cases, we believe the simple water ligand model is sufficiently reliable to provide important insights at relatively low cost.

Summary and Conclusions

In an attempt to gain a better understanding of the activity of Cu–ZSM-5 as a catalyst for the NO decomposition and selective catalytic reduction reactions, we have begun to examine the interaction of zeolite-bound Cu ions with NO and CO. Because the actual Cu–ZSM-5 system is very complex on an atomic scale, small molecule models, including $Cu(H_2O)_x^{n+}$, $Cu(H_2O)_xCO^{n+}$, and $Cu(H_2O)_xNO^{n+}$ ($x = 0–4$, $n = 0–3$), have

been used to represent the real system. The essential assumption of this model is that the bridge oxygens that form the anchor points for Cu ions within zeolites can be adequately represented by a set of water ligands. Water ligands obviously do not incorporate the structural and electronic complexities of real zeolites. They do benefit from simplicity, however, and preliminary results indicate that in most cases they do capture the essential features of the interaction between bridge oxygens and a Cu ion. The simple water ligand model has been exploited here to gain a considerable amount of useful information about the binding of Cu ions within zeolites and the interaction of these Cu ions with NO and CO.

First, Cu^+ and Cu^{2+} are both found to interact with H_2O ligands (or bridge oxygens) in an essentially ionic fashion. Cu^{2+} shows a strong preference for high coordination numbers and thus is more likely to bind in 4-fold or higher coordination sites within ZSM-5. In contrast, Cu^+ prefers, or at least tolerates, lower coordination numbers and is more likely to bind in 2-fold coordination sites, although no energetic penalty is incurred for choosing higher coordination. Essentially the same results hold when CO or NO is bound to the ions.

Second, CO is found to bind to Cu^{2+}, but the bonding interaction is weaker than that between Cu^{2+} and H_2O. Thus, CO is not expected to be able to displace H_2O ligands (or bridge oxygens) from the Cu^{2+} coordination sphere, and zeolite-bound Cu^{2+} may not always be able to bind CO. In contrast, Cu^+ has an approximately equal affinity for CO and H_2O ligands, and Cu^+ within zeolites should be able to readily exchange CO and bridge oxygens in its coordination sphere. Cu^0 also exhibits some affinity for CO, but the binding of $CuCO^0$ to H_2O is very weak, and a $CuCO^0$ moiety is unlikely to be stable within a zeolite. The C–O bond length is virtually unchanged from the free molecule when bound on Cu^+ but is significantly shortened on Cu^{2+} and lengthened on Cu^0. The C–O vibrational frequencies are predicted to follow the trend $CuCO^{2+} > CuCO^+ > CuCO^0$.

Third, NO is found to bind to Cu^{2+}, Cu^+, and Cu^0. In the first case, the bonding is characterized by the transfer of an electron from NO to the Cu^{2+} center and can best be represented as $[Cu(I)–(N\equiv O^+)]$. In the second case, the bonding is primarily dative, and can best be represented as $[Cu(I)–^2(N=O^\bullet)]$, with the unpaired electron localized primarily on NO. In the last case, the bonding is characterized by the transfer of an electron from Cu^0 to the NO ligand and can be represented as $[Cu(I)–^{1,3}(N=O^-)]$, where the singlet and triplet states are close in energy and arise from parallel or paired alignments of two electrons centered on NO. Use of the Cu oxidation state to describe these three bonding situations is clearly ambiguous, and we prefer to use the nomenclature $\{CuNO\}^{10}$, $\{CuNO\}^{11}$, and $\{CuNO\}^{12}$ to describe the systems that have been modeled by $CuNO^{2+}$, $CuNO^+$, and $CuNO^0$ complexes, respectively. The increased localization of unpaired electron density on the nitrogen centers in the latter two cases suggests that these systems may be activated toward further chemistry, such as interaction with another NO molecule or with an olefin.

Fourth, the binding energy of NO to Cu is sensitive both to the CuNO "oxidation state" and to the coordination number of the metal ion. NO binds more strongly to Cu^{2+} than does CO or H_2O, and the $\{CuNO\}^{10}$ unit should be readily generated within Cu-exchanged zeolites and should be fairly robust to cleavage to Cu^{2+} and NO. Cu^+ binds NO, CO, and H_2O equally well, and the $\{CuNO\}^{11}$ unit should be readily formed (and cleaved) within Cu-exchanged zeolites. Cu^0 also binds NO reasonably strongly, and it may be possible to generate a $\{CuNO\}^{12}$ unit within zeolites, perhaps by reduction of the other

Schneider et al.

systems. While the $Cu^{2+}-NO$ bond is robust with respect to fragmentation into Cu^{2+} and NO, it is thermodynamically unstable with respect to fragmentation into Cu^+ and NO^+. As the Cu coordination number increases, the systems become increasingly kinetically stable, and they may become thermodynamically stable in more realistic coordination environments. However, NO does have the potential to serve as a one electron reductant for Cu^{2+} within a zeolite.

While the application of the H_2O model to a specific zeolite, such as Cu–ZSM-5, is obviously speculative, we believe that the results obtained here are an encouraging step toward a better fundamental understanding of the catalytic activity of this complex system. The implications of these observations are being further investigated in our laboratories.

References and Notes

(1) (a) Iwamoto, M.; Yokoo, S.; Sakai, S.; Kagawa, S. *J. Chem. Soc., Faraday Trans. 1* **1981**, 1629. (b) Iwamoto, M.; Furukawa, H.; Mine, Y.; Uemura, F.; Mikuriya, S.; Kagawa, S. *J. Chem. Soc. Chem. Commun.* **1986**, 1272. (c) Iwamoto, M.; Yahiro, H.; Tanda, K.; Mizuno, M.; Mine, Y.; Kagawa, S. *J. Phys. Chem.* **1991**, *95*, 3727.

(2) (a) Li, Y.; Hall, W. K. *J. Phys. Chem.* **1990**, *94*, 6145. (b) Li, Y.; Hall, W. K. *J. Catal.* **1991**, *129*, 202.

(3) Iwamoto, M.; Yahiro, H.; Shundo, Y.; Yu-u, Y.; Mizuno, M. *Shokubai (Catalyst)* **1990**, *32*, 430. (b) Iwamoto, M.; Hamada, H. *Catal. Today* **1991**, *10*, 57. (c) Iwamoto, M.; Mizuno, N. *Proc.—Inst. Mech. Eng.* **1993**, *207*, 23.

(4) Held, W.; Konig, A.; Richter, T.; Puppe, L. *Soc. Aut. Eng.* **1990**, Paper 900496.

(5) Shelef, M. *Chem. Rev.* **1995**, *95*, 209.

(6) Mortier, W. J.; Schoonheydt, R. A. *Prog. Solid State Chem.* **1985**, *16*, 1.

(7) Schoonheydt, R. A. *Catal. Rev.—Sci. Eng.* **1993**, *35*, 129.

(8) Mortier, W. J. *Compilation of Extra-Framework Sites in Zeolites*, Buttersworth, Guildford, 1982.

(9) Anderson, M. W.; Kevan, L. *J. Phys. Chem.* **1987**, *91*, 4174.

(10) (a) Slinkin, A. A.; Kucherov, A. V.; Chuvylkin, N. D.; Korsunov, V. A.; Klyachko, A. L.; Nikishenko, S. B. *Kinet. Katal.* **1990**, *31*, 698. (b) Kucherov, A. V.; Slinkin, A. A. *J. Phys. Chem.* **1989**, *93*, 864. (c) Kucherov, A. V.; Slinkin, A. A.; Kondrat'ev, D. A.; Bondarenko, T. N.; Rubinstein, A. M.; Minachev, Kh. M. *Zeolites* **1985**, *5*, 320.

(11) Larsen, S. C.; Aylor, A.; Bell, A. T.; Reimer, J. A. *J. Phys. Chem.* **1994**, *98*, 11533.

(12) Hamada, H.; Matsubayashi, N.; Shimada, H.; Kintaichi, Y.; Ito, T.; Nishijima, A. *Catal. Lett.* **1990**, *5*, 189.

(13) (a) Liu, D.-J.; Robota, H. *J. Catal. Lett.* **1993**, *21*, 291. (b) Liu, D.-J.; Robota, H. *J. Appl. Catal. B* **1994**, *4*, 155. (c) Liu, D.-J.; Robota, H. J. In *Reduction of Nitrogen Oxide Emissions*, ACS Symposium Series 587; Ozkan, U. S., Aggarwal, S. K., Marcelin, G., Eds.; American Chemical Society: Washington, DC, 1995; Chapter 12, p 147.

(14) Grünert, W.; Hayes, N. W.; Joyner, R. W.; Shpiro, E. S.; Siddiqui, M. R.; Baeva, G. N. *J. Phys. Chem.* **1994**, *98*, 10832.

(15) Shelef, M. *Catal. Lett.* **1992**, *15*, 305.

(16) Hall, W. K.; Valyon, J. *Catal. Lett.* **1992**, *15*, 311.

(17) (a) Kucherov, A. V.; Gerlock, J. L.; Jen, H.-W.; Shelef, M. *J. Phys. Chem.* **1994**, *98*, 4892. (b) Kucherov, A. V.; Gerlock, J. L.; Jen, H.-W.; Shelef, M. *J. Catal.* **1995**, *152*, 63.

(18) Petunchi, J. O.; Marcelin, G.; Hall, W. K. *J. Phys. Chem.* **1992**, *96*, 9967.

(19) Parr, R. G.; Yang, W. *Density-Functional Theory of Atoms and Molecules*; Oxford University Press: Oxford, 1989.

(20) Sauer, J. *Chem. Rev.* **1989**, *89*, 199.

(21) Spoto, G.; Zecchina, A.; Bordiga, S.; Ricchiardi, G.; Martra, G.; Leofanti, G.; Petrini, G. *Appl. Catal. B* **1994**, *3*, 151.

(22) Richter-Addo, G. B.; Legzdins, P. *Metal Nitrosyls*; Oxford University Press: Oxford, 1992.

(23) Baerends, E. J.; Ellis, D. E.; Ros, P. *Chem. Phys.* **1973**, *2*, 41.

(24) Verslius, L.; Ziegler, T. *J. Chem. Phys.* **1988**, *88*, 322.

(25) Vosko, S. H.; Wilk, L.; Nusair, M. *Can. J. Phys.* **1980**, *58*, 1200.

(26) Becke, A. D. *Phys. Rev. A* **1988**, *38*, 3098.

(27) Perdew, J. P. *Phys. Rev. B* **1986**, *33*, 8822.

(28) Ziegler, T.; Rauk, A. *Theor. Chim. Acta* **1977**, *46*, 1.

(29) Fan, L.; Ziegler, T. *J. Chem. Phys.* **1991**, *95*, 7401.

(30) Te Velde, G.; Baerends, E. J. *J. Comput. Phys.* **1992**, *99*, 84.

(31) Delley, B. *J. Chem. Phys.* **1990**, *92*, 508.

(32) Corbin, D. F.; Abrams, L.; Jones, G. A.; Eddy, M. M.; Harrison, W. T. A.; Stucky, G. D.; Cox, D. E. *J. Am. Chem. Soc.* **1990**, *112*, 4821.

(33) Curtiss, L. A.; Jurgens, R. *J. Phys. Chem.* **1990**, *94*, 5509.

(34) (a) Rosi, M.; Bauschlicher, C. W. *J. Chem. Phys.* **1990**, *92*, 1876. (b) Bauschlicher, C. W.; Langhoff, S. R.; Partridge, H. *J. Chem. Phys.* **1991**, *94*, 2068.

(35) Bauschlicher, C. W. *J. Chem. Phys.* **1986**, *84*, 260.

(36) Åkesson, R.; Petterson, L. G. M. *Chem. Phys.* **1994**, *184*, 85.

(37) Boys, S. F.; Bernardi, F. *Mol. Phys.* **1970**, *19*, 553.

(38) Holland, P. M.; Castleman, A. W. *J. Chem. Phys.* **1982**, *76*, 4195.

(39) Magnera, T. F.; David, D. E.; Michl, J. *J. Am. Chem. Soc.* **1989**, *111*, 4100.

(40) Dalleska, N. F.; Honma, K.; Sunderlin, L. S.; Armentrout, P. B. *J. Am. Chem. Soc.* **1994**, *116*, 3519.

(41) Cotton, F. A.; Wilkinson, G. *Advanced Inorganic Chemistry*, 4th ed., Wiley: New York, 1980.

(42) Huang, Y. *J. Am. Chem. Soc.* **1973**, *95*, 6636.

(43) (a) Sodupe, M.; Bauschlicher, C. W.; Lee, T. J. *Chem. Phys. Lett.* **1992**, *189*, 266. (b) Barnes, L. A.; Rosi, M., Bauschlicher, C. W. *J. Chem. Phys.* **1990**, *93*, 609.

(44) Merchán, M.; Nebot-Gil, I.; González-Luque, R.; Ortí, E. *J. Chem. Phys.* **1987**, *87*, 1690.

(45) Meyer, F.; Chen, Y.-M.; Armentrout, P. B. *J. Am. Chem. Soc.* **1995**, *117*, 4071.

(46) Chemier, J. H. B.; Hampson, C. A.; Howard, J. A.; Mile, B. *J. Phys. Chem.* **1989**, *93*, 114.

(47) Kasai, P. H.; Jones, P. M. *J. Am. Chem. Soc.* **1985**, *107*, 813.

(48) Barone, V. *Chem. Phys. Lett.* **1995**, *233*, 129.

(49) Bauschlicher, C. W. *J. Chem. Phys.* **1994**, *100*, 1215.

(50) (a) Fournier, R. *J. Chem. Phys.* **1995**, *102*, 5396. (b) Fournier, R. *J. Chem. Phys.* **1993**, *99*, 1801. (c) Fournier, R. *J. Chem. Phys.* **1993**, *98*, 8041.

(51) Kohler, M. A.; Cant, N. W.; Wainwright, M. S.; Trimm, D. L. *J. Catal.* **1989**, *117*, 188.

(52) Eisenberg, R.; Meyer, C. D. *Acc. Chem. Res.* **1975**, *8*, 26.

(53) Enemark, J. H.; Feltham, R. D. *Coord. Chem. Rev.* **1974**, *13*, 339.

(54) Ruggiero, C. E.; Carrier, S. M.; Antholine, W. E.; Whittaker, J. W.; Cramer, C. J.; Tolman, W. B. *J. Am. Chem. Soc.* **1993**, *115*, 11285.

(55) Giamello, E.; Murphy, D.; Magnacca, G.; Morterra, C.; Shioya, Y.; Nomura, T.; Anpo, M. *J. Catal.* **1992**, *136*, 510.

(56) Valyon, J.; Hall, W. K. *J. Phys. Chem.* **1993**, *97*, 1204.

(57) Wagman, D. D.; Evans, W. H.; Parker, V. B.; Schumm, R. H.; Halow, I.; Bailey, S. M.; Churney, K. L.; Nuttall, R. L. *J. Phys. Chem. Ref. Data* **1982**, *11*, Suppl. 2.

(58) Hrušák, J.; Koch, W.; Schwarz, H. *J. Chem. Phys.* **1994**, *101*, 3898.

(59) Chiarelli, J. A.; Ball, D. W. *J. Phys. Chem.* **1994**, *98*, 12828.

(60) Gandhi, H. S.; Shelef, M. *J. Catal.* **1973**, *28*, 1.

(61) Hass, K. C.; Schneider, W. F. *J. Phys. Chem.*, submitted for publication.

(62) Herzberg, G. *Molecular Spectra and Molecular Structure. I. Spectra of Diatomic Molecules*, 2nd ed., Van Nostrand Reinhold: New York, 1950.

(63) *CRC Handbook of Chemistry and Physics*, 63rd ed.; Weast, R. C., Ed.; CRC Press: Boca Raton, FL, 1982.

(64) Herzberg, G. *Molecular Spectra and Molecular Structure. II. Infrared and Raman Spectra of Polyatomic Molecules*, Van Nostrand Reinhold: New York, 1945.